



HAL
open science

An asymptotic two layers monodomain model of cardiac electrophysiology in the atria

Yves Coudière, Jacques Henry, Simon Labarthe

► **To cite this version:**

Yves Coudière, Jacques Henry, Simon Labarthe. An asymptotic two layers monodomain model of cardiac electrophysiology in the atria. [Research Report] RR-8593, INRIA. 2014, pp.32. hal-00922717v2

HAL Id: hal-00922717

<https://inria.hal.science/hal-00922717v2>

Submitted on 9 Sep 2014 (v2), last revised 18 Mar 2017 (v4)

HAL is a multi-disciplinary open access archive for the deposit and dissemination of scientific research documents, whether they are published or not. The documents may come from teaching and research institutions in France or abroad, or from public or private research centers.

L'archive ouverte pluridisciplinaire **HAL**, est destinée au dépôt et à la diffusion de documents scientifiques de niveau recherche, publiés ou non, émanant des établissements d'enseignement et de recherche français ou étrangers, des laboratoires publics ou privés.



An Asymptotic Two Layers Monodomain Model of Cardiac Electrophysiology in the Atria

Yves Coudière, Jacques Henry, Simon Labarthe

**RESEARCH
REPORT**

N° 8593

September 2014

Project-Team Carmen



An Asymptotic Two Layers Monodomain Model of Cardiac Electrophysiology in the Atria

Yves Coudière*[†], Jacques Henry*[†], Simon Labarthe^{‡†}

Project-Team Carmen

Research Report n° 8593 — September 2014 — 32 pages

Abstract: Numerical simulations of the cardiac electrophysiology in the atria are often based on the standard bidomain or monodomain equations stated on a two-dimensional manifold. These simulations take advantage of the thinness of the atrial tissue, and their computational costs is reduce, as compared to three-dimensional simulations. However, these models do not take into account the heterogeneities located in the thickness of the tissue, like discontinuities of the fiber direction, although they can be a substrate for atrial arrhythmia. We investigate a two-dimensional model with two coupled, superimposed layers that allows to introduce three-dimensional heterogeneities, but retains a reasonable computational cost. We introduce the mathematical derivation of this model, show its convergence toward the three-dimensional model and give some numerical illustration of its interest. Our model would be an efficient tool to test the influence of three-dimensional fiber direction heterogeneities in reentries or atrial arrhythmia without using three-dimensional models.

Key-words: Cardiac modeling, Atrial model, Surface model, asymptotic analysis

* IMB, Université Bordeaux 1, 351, cours de la Libération - F 33405 TALENCE cedex

[†] Inria Carmen, 200 avenue de la Vieille Tour, 33 405 Talence Cedex, F

[‡] IMB, Université Bordeaux Segalen, 146 Rue Léo Saignat, 33076 Bordeaux

**RESEARCH CENTRE
BORDEAUX – SUD-OUEST**

200 avenue de la Vieille Tour
33405 Talence Cedex

Un modèle monodomaine asymptotique bicouche de l'électrophysiologie cardiaque appliqué aux oreillettes

Résumé : Les simulations numériques de l'activité électrophysiologique cardiaque dans les oreillettes sont souvent basées sur les équations bidomaines ou monodomaines définies sur une variété. Cette modélisation tire avantage de la faible épaisseur des tissus auriculaires, et permettent des réductions importantes de coûts numériques, comparativement aux modèles tridimensionnels. Cependant, les hétérogénéités localisées dans l'épaisseur du tissu, telles que des discontinuités dans la distribution des fibres, ne sont pas prise en compte par ces modèles, alors qu'elles peuvent être des déclencheurs d'arythmies auriculaires. Nous étudions un modèle bicouche composé de deux couches superposées qui permet de prendre en compte des hétérogénéités tridimensionnelles, tout en conservant une charge numérique raisonnable. Nous introduisons la dérivation mathématique de ce modèle, nous montrons sa convergence vers un modèle tridimensionnel équivalent et nous donnons quelques illustrations numériques de son intérêt. Notre modèle pourrait être un outil efficace pour étudier l'influence de la distribution tridimensionnelle des fibres musculaires sur l'apparition de réentrées ou d'arythmies, sans utiliser de modèle tridimensionnel.

Mots-clés : Modélisation cardiaque, modèle auriculaire, modèle surfacique, Analyse asymptotique

1 Introduction

Modeling the electrophysiology of cardiac tissues is considered an investigation tool for clinical and fundamental research. Theoretical studies and numerical simulations have been recognized an efficient way to improve our knowledge of arrhythmia genesis [Zemlin et al., 2009, Haissaguerre et al., 2007], perpetuation [Cain, 2007], and ablation efficiency [ROTTER et al., 2007, Nagaiah et al., 2013].

In three-dimensional tissues, the propagation of the action potential is modeled by the monodomain or bidomain systems of equations. These are reaction-diffusion equations, where the reaction represents the ionic function of the tissue and the diffusion accounts for the diffusion of electrical charges.

Models of the propagation of the action potential through the atria are often formulated as monodomain or bidomain systems of equations on bi-dimensional manifolds [Haissaguerre et al., 2007, ROTTER et al., 2007, Dang et al., 2005]. Such surface models take advantage of the thinness of the atria with respect to the length scale of the heart, and drastically reduce the numerical cost of their resolution, hence allowing thorough in-silico investigations of atrial arrhythmias. These surface models approximate the first term of the asymptotic expansion (with respect to the thickness) of the three-dimensional equations, as presented in section 4. The thickness itself is not part of the final model, since it is assumed to vanish.

On the other hand, there exists structural and functional heterogeneities within the atria, such as fiber direction discontinuities through the wall. For instance, several superimposed layers with different fiber directions were described in the atrial wall or in the ostium zones of the pulmonary veins [Ho et al., 2001, 1999, Hocini et al., 2002, Saito et al., 2000]. In these anatomical regions, the transition of fibers directions between layers can be very abrupt. These abrupt transitions can trigger complex propagation patterns [Vetter et al., 2005] (and also Figure 3), and are suspected to be a substrate for re-entries or arrhythmia [Hocini et al., 2002, Ho et al., 2002, Nattel, 2002]. Functional transmural heterogeneities have also been demonstrated during atrial fibrillation [Eckstein et al., 2011]. The usual surface models do not account for such heterogeneities. The model proposed in [Chapelle et al., 2013] is a surface bidomain system of equations with anisotropic conductivity derived from fiber direction varying smoothly through the atrial wall. This derivation is based on a rigorous mathematical study, including curvature effects. Although it seems to be an improvement over the usual models, it still does not account for the complex propagation pattern mentioned above.

In order to overcome this difficulty, models with several surface layers have been proposed [dos Santos and Dickstein, 2003, Jacquemet, 2004, Gharaviri et al., 2012]. The main idea is to include the structural heterogeneities of leading importance while keeping the convenience of a surface model. However, the mathematical foundations of these models have not been studied in depth, and the physiological assumptions on which they rely are still unclear.

In this paper, we show that a special attention must be paid to the physiological scaling of the equations. We notably show that the balance between the reaction terms and transverse diffusion (conductivity through the wall) entirely determines the regime of the solutions. If transverse diffusion dominates, then the usual surface models are sufficient to represent the average behavior of the action potential. But if reaction cannot be neglected compared to transverse diffusion, then complex patterns (Figure 3) are observed, and the transmural effects must not be neglected. This is typically the case during electrical depolarization for human atria, as discussed in section 3.2. To account for this regime, we first introduce the second order term in the asymptotic expansion of the solutions, instead of simply the first one. But this would not yield a model that clearly differentiates between different layers. Hence we propose a model that represents the evolution of the transverse averages of the transmembrane voltage in each of the tissue's layers. Consequently, we design a surface model with two layers having distinct conductivity tensor and electrophysiology source function. With this new vision, we can see how the thickness appears in the equations, and we account for the main structural and functional observations described above.

For a slab of tissue with two distinct layers, the model is formally derived from the three-dimensional monodomain equations in two steps: the second order completion of the usual surface model is first

computed, and then the averages of this second order model are shown to solve a set of two coupled surface monodomain equations, associated to the two layers of the tissue. The error between this two-surfaces model and the transverse averages of the three-dimensional model is rigorously proved to be of order ε^3 , where ε is the aspect ratio of the atria. Some numerical results illustrate the good behavior of this model.

The paper is organized as follows. Section 2 briefly recalls the monodomain equations. Section 3 introduces the geometrical framework of our paper, introduces the small parameter ε , explains the scaling of the equations and discusses the different regime observed. It justifies the fact that the thickness cannot be neglected during the depolarization process in the atria. Section 4 presents a derivation of the second order surface model similar (but one order more accurate) to the usual surface models, and gives the corresponding error estimate. Section 5 proposes a derivation of our two layers model with two systems of monodomain equations formulated on a surface, and also proves the corresponding error estimate. Section 6 is devoted to the numerical illustrations. The conclusions are discussed in section 7.

2 The monodomain equations

The bidomain equations, first introduced in [Clerc, 1976, Tung, 1978], is a degenerate system of two anisotropic reaction-diffusion equations coupled to a set of ordinary differential equations. They describe the evolution of the intra- and extra-cellular potential at the tissue scale [Krassowska and Neu, 1993], and they can mimic complex phenomena such as virtual electrodes [Sepulveda et al., 1989]. Under the equal anisotropy ratio assumption the system can be reduced to the single monodomain reaction-diffusion equation. In the vast majority of applications, the solutions to this monodomain equation are very close to the solution to the bidomain equation [Potse et al., 2006]. The models proposed and discussed in this paper are based on the monodomain approximation although it is straightforward to derive a bidomain version of them.

Let Ω be an open subset of \mathbb{R}^3 and (u, w) be the solution of the monodomain equations, that read

$$A(C\partial_t u + f(u, w)) = \operatorname{div}(\sigma \nabla u) \quad \text{in } (0, +\infty) \times \Omega, \quad (1)$$

$$\partial_t w + g(u, w) = 0 \quad \text{in } (0, +\infty) \times \Omega \quad (2)$$

where the parameters A , C and σ are, respectively, the ratio of surface of membrane to total volume (in cm^{-1}), the membrane capacitance (in μFcm^{-2}) and the conductivity (in mScm^{-2}). The unknowns are the transmembrane potential $u(t, x) \in \mathbb{R}$ (in mV) and the m variables $w(t, x) \in \mathbb{R}^m$ that describe the electrophysiological state of the membrane. The evolution of the electrophysiological state w is modeled by the functions $f: \mathbb{R} \times \mathbb{R}^m \rightarrow \mathbb{R}$ and $g: \mathbb{R} \times \mathbb{R}^m \rightarrow \mathbb{R}^m$.

The domain Ω represents the myocardial domain. In this domain, the cardiomyocytes organize into fibers, that in turn organize into laminae. This cardiac tissue is modeled as a homogenized continuous medium with heterogeneous and anisotropic electrical conductivity σ that reads:

$$\forall x \in \bar{\Omega}, \quad \sigma(x) = \sum_{i=1}^3 \sigma_i v_i(x) v_i^T(x)$$

where (v_1, v_2, v_3) is the orthonormal basis in \mathbb{R}^3 aligned on the fiber and laminae directions and $0 < \underline{\sigma} := \sigma_3 \leq \sigma_2 \leq \sigma_1 := \bar{\sigma}$ are constant parameters. As a consequence, the diffusion operator is bounded and uniformly elliptic:

$$\forall x \in \bar{\Omega}, \quad \underline{\sigma} |\xi|^2 \leq \xi^T \sigma(x) \xi = \sum_{i=1}^3 \sigma_i |\xi_i|^2 \leq \bar{\sigma} |\xi|^2.$$

Equations (1) and (2) are supplemented with the Neumann boundary condition

$$\sigma \nabla u \cdot n = 0 \quad \text{in } (0, +\infty) \times \partial\Omega \quad (3)$$

that models an electrically insulated heart, together with the initial condition

$$u(0, x) = u^0(x), \quad w(0, x) = w^0(x) \quad \text{a.e. } x \in \Omega. \quad (4)$$

We will assume that the monodomain equations (1) and (2) with the boundary and initial conditions (3) and (4) have a unique solution u and w defined for a.e. $x \in \Omega$ and for all $t > 0$. We will furthermore assume that this solution is regular enough to carry out all our proofs.

For instance, assuming that f and g are uniform Lipschitz functions, the unique weak solution to the monodomain equations is given by some functions u and w such that: $u \in L^2(0, T; H^1(\Omega))$ and $\partial_t u \in L^2(0, T; (H^1(\Omega))')$, and $w \in L^2(0, T; L^2(\Omega))$ and $\partial_t w \in L^2(0, T; L^2(\Omega))$, for any $T > 0$ (see [Bendahmane and Karlsen, 2006]).

3 Transmural discontinuities of the fiber structure and dimensional analysis

3.1 A two-layers slab of myocardium

We consider an ideal slab of cardiac tissue Ω composed of two layers with the same thickness $h > 0$ and distinct fiber directions, specifically $\Omega = \omega \times (-h, h) \subset \mathbb{R}^3$, where ω is an open bounded subset of \mathbb{R}^2 and the two layers are $\Omega^{(1)} = \omega \times (0, h)$ and $\Omega^{(2)} = \omega \times (-h, 0)$. The boundary of each layer is split into the external boundary and the interface between the layers, namely $\Gamma^{(k)} = \partial\Omega^{(k)} \cap \partial\Omega$ for $k = 1, 2$ and $\Sigma = \omega \times \{0\}$. The coordinates of a point $x \in \Omega$ are written $x = (x', z)$ with $x' \in \omega$ and $-h < z < h$. We assume that the fibers have a constant direction in each layer, specifically, for $k = 1, 2$,

$$v_1^{(k)} = \begin{pmatrix} \cos(\theta^{(k)}) \\ \sin(\theta^{(k)}) \\ 0 \end{pmatrix}, \quad v_2^{(k)} = \begin{pmatrix} -\sin(\theta^{(k)}) \\ \cos(\theta^{(k)}) \\ 0 \end{pmatrix}, \quad v_3^{(k)} = \begin{pmatrix} 0 \\ 0 \\ 1 \end{pmatrix} \quad (5)$$

where $\theta^{(1)}$ and $\theta^{(2)}$ are fixed angles. Consequently, the conductivity tensors in the layers read

$$\sigma^{(k)} = \underbrace{\sum_{j=1}^2 \sigma_j^{(k)} v_j^{(k)} v_j^{(k)T}}_{=\sigma'^{(k)}} + \sigma_3^{(k)} v_3^{(k)} v_3^{(k)T} \quad \text{for } k = 1, 2. \quad (6)$$

where $\sigma'^{(k)}$ is the 2×2 longitudinal conductivity tensor associated to the layer number k .

We denote by σ the conductivity tensor in Ω , defined by $\sigma(x) = \sigma^{(1)}(x)$ if $x \in \Omega^{(1)}$ and $\sigma(x) = \sigma^{(2)}(x)$ if $x \in \Omega^{(2)}$. Hence, given initial data u^0 and w^0 in Ω , the propagation of the action potential in Ω is uniquely described by the monodomain equations (1) and (2) in Ω with the piecewise constant conductivity σ , the boundary condition (3) on $\partial\Omega$, and the initial condition (4). We denote by $(u^{(k,0)}, w^{(k,0)})$ the restriction of the initial data (u^0, w^0) to the layer $\Omega^{(k)}$, and by $(u^{(k)}, w^{(k)})$ the restriction of the solution (u, w) to $\Omega^{(k)}$. Each of these restrictions solves the monodomain equations written in the subdomain $\Omega^{(k)}$ ($k = 1, 2$), that read

$$A \left(\mathcal{C} \partial_t u^{(k)} + f(u^{(k)}, w^{(k)}) \right) = \operatorname{div}_{x'} \left(\sigma'^{(k)} \nabla_{x'} u^{(k)} \right) + \sigma_3^{(k)} \partial_{zz} u^{(k)}, \quad (7)$$

$$\partial_t w^{(k)} + g(u^{(k)}, w^{(k)}) = 0 \quad (8)$$

for $t > 0$ and $x \in \Omega^{(k)}$ with the boundary and transmission conditions

$$\sigma^{(k)} \nabla u^{(k)} \cdot n = 0 \quad \text{on } \Gamma^{(k)}, \quad k = 1, 2, \quad (9)$$

$$\sigma^{(1)} \nabla u^{(1)} \cdot n_\Sigma = \sigma^{(2)} \nabla u^{(2)} \cdot n_\Sigma, \quad u^{(1)} = u^{(2)} \quad \text{on } \Sigma \quad (10)$$

where n is the unit normal to $\partial\Omega$ outward of Ω and n_Σ is the unit normal to Σ pointing from $\Omega^{(2)}$ to $\Omega^{(1)}$, and the initial conditions

$$u^{(k)}(0, x) = u^{(k,0)}(x), \quad w^{(k)}(0, x) = w^{(k,0)}(x) \quad \text{a.e. } x \in \Omega^{(k)}, \quad k = 1, 2. \quad (11)$$

3.2 Dimensionless scaling of the equations

In order to discuss the relative importance of the various terms, the monodomain equations are recast in a dimensionless system of equations following the strategies proposed in [Colli Franzone et al., 1990, Keener, 1991, Rioux, 2012] for cardiac tissues. Given some time and space characteristic lengths t_0 and x_0 and given the thickness $h > 0$ of the two layers, we first define the dimensionless variables

$$\bar{x} = \frac{x'}{x_0}, \quad \bar{t} = \frac{t}{t_0} \quad \text{and} \quad \bar{z} = \frac{z}{h}.$$

For instance, to observe the whole action potential, we will set the length scale to $x_0 = 1\text{cm}$ and the time scale to $t_0 = 400\text{ms}$, because they are the typical extent of atrial structures such as pulmonary veins and the duration of an action potential. The two-layers domain $\Omega = \omega \times (-h, h)$ is mapped to $\bar{\omega} \times (-1, 1)$ where $\bar{\omega} = \frac{1}{x_0}\omega \subset \mathbb{R}^2$. The physical quantities are rescaled as follows:

$$\begin{aligned} \bar{u}^{(k)}(\bar{t}, \bar{x}, \bar{z}) &= \frac{u^{(k)}(t, x', z) - u_r}{\delta u}, \\ \bar{\sigma}^{(k)} &= \frac{1}{\sigma_0} \sigma'^{(k)}, \quad \bar{\sigma}_3^{(k)} = \frac{\sigma_3^{(k)}}{\sigma_0}, \\ \bar{f}(\bar{u}^{(k)}, \bar{w}^{(k)}) &= \frac{1}{f_0} f(u^{(k)}, w^{(k)}), \quad \text{and} \quad \bar{g}(\bar{u}^{(k)}, \bar{w}^{(k)}) = t_0 g(u^{(k)}, w^{(k)}) \end{aligned}$$

where we use the typical amplitude of an action potential δu , the resting potential u_r , the maximum value of the sodium current f_0 (specifically the maximum value reached by the function f) and the characteristic conductivity scale σ_0 . The monodomain equations for the two-layers domain finally read

$$\begin{aligned} AC \frac{x_0^2}{\sigma_0 t_0} \left(\partial_{\bar{t}} \bar{u}^{(k)} + \frac{f_0 t_0}{C \delta u} \bar{f}(\bar{u}^{(k)}, w^{(k)}) \right) &= \text{div}_{\bar{x}} \left(\bar{\sigma}^{(k)} \nabla_{\bar{x}} \bar{u}^{(k)} \right) + \frac{x_0^2}{h^2} \bar{\sigma}_3^{(k)} \partial_{\bar{z}\bar{z}} \bar{u}^{(k)}, \\ \partial_{\bar{t}} \bar{w}^{(k)} + \bar{g}(\bar{u}^{(k)}, w^{(k)}) &= 0 \end{aligned}$$

for $t > 0$ and (\bar{x}, \bar{z}) in the domains $\bar{\Omega}^{(1)} := \bar{\omega} \times (0, 1)$ and $\bar{\Omega}^{(2)} := \bar{\omega} \times (-1, 0)$. The boundary and transmission conditions (9) and (10) remain unchanged but are now stated on $\bar{\Gamma}^{(k)} = \partial\bar{\Omega}^{(k)} \cap \partial\bar{\Omega}$ and $\bar{\Sigma} = \bar{\omega} \times \{0\}$.

As a consequence, the dimensionless numbers

$$\alpha = AC \frac{x_0^2}{\sigma_0 t_0}, \quad \beta = \frac{f_0 t_0}{C \delta u} \quad \text{and} \quad \varepsilon = \frac{h}{x_0}$$

characterize the solutions. The order of magnitude of each of the physical quantities are set according to values usual for cardiac electrophysiology (see table 3.2 for some values of the conductivities):

$$\begin{aligned} A &= 1000\text{cm}^{-1}, \quad C = 1\mu\text{Fcm}^{-2}, \quad \delta u = 100\text{mV}, \\ f_0 &= 100\mu\text{Acm}^{-2}, \quad \sigma_0 = 1.5\text{mScm}^{-1}. \end{aligned}$$

The orders of magnitude of the observation scales (t_0 and x_0) are then set to $x_0 = 1\text{cm}$, $t_0 = 400\text{ms}$, and consequently, the dimensionless parameters α and β are $\alpha = 1.67$, and $\beta = 400$. Since we consider

	Article	1	2	3			4	
Intracellular	σ_1	3.0	3.0	1.741	1.7	2.4	2.0	3.0
	$\sigma_2 = \sigma_3$	0.3	0.3	0.475	0.19	0.24	0.4167	0.315
Extracellular	σ_1	3.0	3.0	3.906	6.2	4.8	2.5	2.0
	$\sigma_2 = \sigma_3$	1.2	1.2	1.97	2.4	2.2	1.25	1.35
Monodomain	σ_1	1.5	1.5	1.204	1.33	1.6	1.11	1.2
	$\sigma_2 = \sigma_3$	0.24	0.24	0.383	0.18	0.22	0.31	0.25

Table 1: Electrical conductivities taken from the literature (mScm^{-1} – monodomain conductivities are the half of the harmonic averages of bidomain ones). Article 1: [Boulakia et al., 2010], article 2: [Potse et al., 2006], article 3: [Clements et al., 2004] (review), and article 4: [Colli Franzone et al., 1990].

layers of cardiac tissue, the important quantity is the aspect ratio $\varepsilon = h/x_0$, assumed to be small. The dimensionless monodomain equations in each layer finally read:

$$\begin{aligned} \alpha \left(\partial_t \bar{u}^{(k)} + \beta \bar{f}(\bar{u}^{(k)}, w^{(k)}) \right) &= \text{div}_{\bar{x}} \left(\bar{\sigma}^{(k)} \nabla_{\bar{x}} \bar{u}^{(k)} \right) + \frac{\bar{\sigma}_3^{(k)}}{\varepsilon^2} \partial_{\bar{z}\bar{z}} \bar{u}^{(k)}, \\ \partial_t \bar{w}^{(k)} + \bar{g}(\bar{u}^{(k)}, w^{(k)}) &= 0 \end{aligned}$$

and every parameter is fixed and of order 1 except ε and β . According to our analysis, the transverse diffusion $\partial_{\bar{z}\bar{z}} \bar{u}^{(k)}$ dominates the reaction terms whenever $\beta \varepsilon^2 \ll 1$. In the next section, we will derive an asymptotic model for $\varepsilon \rightarrow 0$, consequently in the dominant transverse diffusion regime.

Remark 1 *The documented thickness of human atrial tissues is small, but it remains of order $h = 0.1\text{cm}$. For that values, ε is not small enough to obtain an accurate approximation of the observation.*

For this reason, we develop a higher order asymptotic model in section 5.

During the repolarization, the ionic currents are far less intense, so that the asymptotic regime applies quite well for human atria (β decreases, so that $\beta \varepsilon^2 \leq 1$).

4 The asymptotic model with one layer

4.1 Formal derivation of the equations

In this section, we recall how to derive the usual two-dimensional surface model of the atria, that has been used in several numerical studies (see e.g. [Haissaguerre et al., 2007, ROTTER et al., 2007]). According to the previous section (dropping the $\bar{\cdot}$ above the dimensionless quantities and stressing the dependence on ε by a subscript), the three-dimensional dimensionless problem reads

$$\alpha \left(\partial_t u_\varepsilon^{(k)} + \beta f \left(u_\varepsilon^{(k)}, w_\varepsilon^{(k)} \right) \right) = \text{div}_x \left(\sigma^{(k)} \nabla_x u_\varepsilon^{(k)} \right) + \frac{\sigma_3^{(k)}}{\varepsilon^2} \partial_{zz} u_\varepsilon^{(k)}, \quad (12)$$

$$\partial_t w_\varepsilon^{(k)} + g \left(u_\varepsilon^{(k)}, w_\varepsilon^{(k)} \right) = 0 \quad (13)$$

for $k = 1, 2, t > 0$ and $(x, z) \in \Omega^{(k)}$. The boundary and transmission conditions become

$$\sigma^{(1)} \nabla_x u_\varepsilon^{(1)} \cdot n = 0 \quad \text{in } \partial\omega \times (0, 1) \quad \text{and} \quad \sigma_3^{(1)} \partial_z u_\varepsilon^{(1)} = 0 \quad \text{in } \omega \times \{1\}, \quad (14)$$

$$\sigma^{(2)} \nabla_x u_\varepsilon^{(2)} \cdot n = 0 \quad \text{in } \partial\omega \times (-1, 0) \quad \text{and} \quad \sigma_3^{(2)} \partial_z u_\varepsilon^{(2)} = 0 \quad \text{in } \omega \times \{-1\}, \quad (15)$$

$$\sigma_3^{(1)} \partial_z u_\varepsilon^{(1)} = \sigma_3^{(2)} \partial_z u_\varepsilon^{(2)}, \quad u_\varepsilon^{(1)} = u_\varepsilon^{(2)} \quad \text{in } \omega \times \{0\}, \quad (16)$$

and we assume, for the sake of simplicity, that the initial data are independent of $k \in \{1, 2\}$ and of $z \in (-1, 1)$, specifically:

$$u_\varepsilon^{(k)}(0, x, z) = u^0(x), \quad w_\varepsilon^{(k)}(0, x, z) = w^0(x) \quad \text{in } \Omega^{(k)}, \quad k = 1, 2, \quad (17)$$

where the functions $u^0(x)$ and $w^0(x)$ are given functions of $x \in \omega$. We consider the following expansion of $u_\varepsilon^{(k)}$ and $w_\varepsilon^{(k)}$:

$$u_\varepsilon^{(k)} = u_0^{(k)} + \varepsilon^2 u_1^{(k)} + \varepsilon^4 u_2^{(k)} + o(\varepsilon^4), \quad w_\varepsilon^{(k)} = w_0^{(k)} + \varepsilon^2 w_1^{(k)} + o(\varepsilon^2),$$

for all $t \geq 0$, so that, in particular,

$$\begin{aligned} u_0^{(k)}(0, x, z) &= u^0(x), & u_j^{(k)}(0, x, z) &= 0 \quad \text{for } j \geq 1, \\ w_0^{(k)}(0, x, z) &= w^0(x), & w_j^{(k)}(0, x, z) &= 0 \quad \text{for } j \geq 1. \end{aligned}$$

We introduce this expansion in the system of eqs. (12) and (13) and identify the coefficients having the same order with respect to ε^2 . The coefficient of order $1/\varepsilon^2$ yields the equation $\partial_{zz} u_0^{(k)} = 0$ for $k = 1, 2$ together with the boundary and transmission conditions for $u_0^{(k)}$, in the direction z ,

$$\begin{aligned} \partial_z u_0^{(1)}(t, x, 1) &= \partial_z u_0^{(2)}(t, x, -1) = 0, \\ \sigma_3^{(1)} \partial_z u_0^{(1)}(t, x, 0) &= \sigma_3^{(2)} \partial_z u_0^{(2)}(t, x, 0), \quad u_0^{(1)}(t, x, 0) = u_0^{(2)}(t, x, 0). \end{aligned}$$

These equations easily show that $u_0^{(1)}(t, x, z) = u_0^{(2)}(t, x, z) := u_0(t, x)$ is a function independent of z , defined for $t \geq 0$ and a.e. $x \in \omega$. We can write a second order approximation of the functions f and g :

$$\begin{aligned} f(u_\varepsilon^{(k)}, w_\varepsilon^{(k)}) &= f(u_0, w_0^{(k)}) + \varepsilon^2 \nabla f(u_0, w_0^{(k)}) \cdot (u_1^{(k)}, w_1^{(k)}) + o(\varepsilon^2), \\ g(u_\varepsilon^{(k)}, w_\varepsilon^{(k)}) &= g(u_0, w_0^{(k)}) + \varepsilon^2 \nabla g(u_0, w_0^{(k)}) \cdot (u_1^{(k)}, w_1^{(k)}) + o(\varepsilon^2). \end{aligned}$$

We then get the following equation on $u_1^{(k)}$, for $k = 1, 2$, identifying the coefficients of the terms of order ε^0 .

$$\sigma_3^{(k)} \partial_{zz} u_1^{(k)} = \alpha \left(\partial_t u_0 + \beta f(u_0, w_0^{(k)}) \right) - \operatorname{div}_x \left(\sigma^{(k)} \nabla_x u_0 \right), \quad (18)$$

$$\partial_t w_0^{(k)} + g(u_0, w_0^{(k)}) = 0, \quad (19)$$

with the boundary and interface conditions (14) to (16) on $u_1^{(k)}$. The evolution of $w_0^{(k)}$ only depends on the function $(t, x, z) \mapsto g(u_0(t, x), \cdot)$, which is independent of z . Since $w_\varepsilon^{(k)}(0, x, z) = w^0(x)$ is independent of z and of $k = 1, 2$, the functions $w_0^{(k)}$ are independent of z for all time $t > 0$ and have the same value, solution to equation (19), that we denote by $w_0(t, x) := w_0^{(1)}(t, x, z) = w_0^{(2)}(t, x, z)$ for all $t \geq 0$ and a.e. $x \in \omega$. Afterwards, we integrate the equation (18) on $u_1^{(k)}$ along z and use equations (14) and (15) to get

$$-\sigma_3^{(1)} \partial_z u_1^{(1)}(\cdot, 0) = \alpha \left(\partial_t u_0 + \beta f(u_0, w_0) \right) - \operatorname{div}_x \left(\sigma^{(1)} \nabla_x u_0 \right), \quad (20)$$

$$\sigma_3^{(2)} \partial_z u_1^{(2)}(\cdot, 0) = \alpha \left(\partial_t u_0 + \beta f(u_0, w_0) \right) - \operatorname{div}_x \left(\sigma^{(2)} \nabla_x u_0 \right). \quad (21)$$

Finally, we add these two equations and use the transmission condition (16) to obtain the following system of equations on (u_0, w_0) :

$$\alpha(\partial_t u_0 + \beta f(u_0, w_0)) = \operatorname{div}_x(\sigma^m \nabla_x u_0), \quad (22)$$

$$\partial_t w_0 + g(u_0, w_0) = 0, \quad (23)$$

with the boundary condition $\sigma^m \nabla_x u_0 \cdot n = 0$ on $\partial\omega$ and for $t > 0$ and initial condition $u_0(0, x) = u^0(x)$ and $w_0(0, x) = w^0(x)$ in ω . We denote by $\sigma^m = \frac{\sigma^{(1)} + \sigma^{(2)}}{2}$ the arithmetic average of the conductivity matrices in both layers. For the sake of simplicity in the computations below, we also introduce the notation $\sigma^d = \frac{\sigma^{(1)} - \sigma^{(2)}}{2}$.

Remark 2 Equations (22) and (23), defined on the surface ω , independent of ε , and with a conductivity matrix averaged in the thickness, are the usual surface model for the atria. It has been rigorously derived for instance in [Chapelle et al., 2013].

Now, note that the right-hand side of equations (18) is independent of z . Using equation (22), it is equal to $\operatorname{div}_x(\sigma^m \nabla_x u_0) - \operatorname{div}_x(\sigma^{(k)} \nabla_x u_0) = \pm \operatorname{div}_x(\sigma^d \nabla_x u_0)$, and to the right-hand side of equations (20) and (21). Consequently, the functions $z \mapsto u_1^{(k)}(t, x, z)$ are quadratic in z . There exists $a^{(k)}, b^{(k)}$ and $c^{(k)}$ such that

$$u_1^{(k)}(t, x, z) = a^{(k)}(t, x)z^2 + b^{(k)}(t, x)z + c^{(k)}(t, x)$$

and the left-hand side of equations (18), (20), and (21) are, respectively, $2a^{(k)}\sigma_3^{(k)}$, $-\sigma_3^{(1)}b^{(1)}$ and $\sigma_3^{(2)}b^{(2)}$. Consequently, we can define

$$b := \operatorname{div}_x(\sigma^d \nabla_x u_0) = -2a^{(1)}\sigma_3^{(1)} = \sigma_3^{(1)}b^{(1)} = 2a^{(2)}\sigma_3^{(2)} = \sigma_3^{(2)}b^{(2)}.$$

The transmission condition on $u_1^{(k)}$ on ω yields $c^{(1)} = c^{(2)} := c$ and we can summarize the results as follows: we have

$$u_1^{(k)} = \frac{b}{\sigma_3^{(k)}}z \left(1 - \frac{|z|}{2}\right) + c \quad \text{where } b = \operatorname{div}_x(\sigma^d \nabla_x u_0), \quad (24)$$

and $c = c(t, x)$ is an unknown function. We denote by $\bar{u}_1^{(k)}$ the averages of $u_1^{(k)}$ through each layer $k = 1, 2$ and find that

$$\bar{u}_1^{(1)} := \int_0^1 u_1^{(1)}(\cdot, z) dz = c + \frac{1}{3} \frac{b}{\sigma_3^{(1)}} \quad \text{and} \quad \bar{u}_1^{(2)} := \int_{-1}^0 u_1^{(2)}(\cdot, z) dz = c - \frac{1}{3} \frac{b}{\sigma_3^{(2)}}.$$

As a consequence, we have the relations

$$\bar{u}_1 := \frac{\bar{u}_1^{(1)} + \bar{u}_1^{(2)}}{2} = c + \frac{1}{6} b \frac{\sigma_3^{(2)} - \sigma_3^{(1)}}{\sigma_3^{(2)} \sigma_3^{(1)}}, \quad \frac{\bar{u}_1^{(1)} - \bar{u}_1^{(2)}}{2} = \frac{1}{6} b \frac{\sigma_3^{(2)} + \sigma_3^{(1)}}{\sigma_3^{(2)} \sigma_3^{(1)}} := \frac{1}{3} \frac{b}{\sigma_3^h},$$

where \bar{u}_1 denotes the average of $u_1^{(k)}$ through the whole thickness of the tissue and $\sigma_3^h = 2 \frac{\sigma_3^{(1)} \sigma_3^{(2)}}{\sigma_3^{(1)} + \sigma_3^{(2)}}$ is the harmonic average of the transverse conductivities. Hence, c can be found if we know \bar{u}_1 . We also denote by \bar{w}_1 the average of $w_1^{(k)}$ through the whole thickness of the tissue, defined by

$$\bar{w}_1 = \frac{1}{2} \left(\int_0^1 w_1^{(1)}(\cdot, z) dz + \int_{-1}^0 w_1^{(2)}(\cdot, z) dz \right).$$

Now, the functions (\bar{u}_1, \bar{w}_1) are solution to the system of equations obtained by identifying the coefficients of order ε^2 in the expansion of $(u^{(k)}, w^{(k)})$. We first get the equations

$$\sigma_3^{(k)} \partial_{zz} u_2^{(k)} = \alpha \left(\partial_t u_1^{(k)} + \beta \nabla f(u_0, w_0) \cdot (u_1^{(k)}, w_1^{(k)}) \right) - \operatorname{div}_x \left(\sigma^{(k)} \nabla_x u_1^{(k)} \right), \quad (25)$$

$$\partial_t w_1^{(k)} + \nabla g(u_0, w_0) \cdot (u_1^{(k)}, w_1^{(k)}) = 0, \quad (26)$$

with the boundary and transmission conditions (14) to (16) on $u_2^{(k)}$. For $k = 1, 2$ and for each $(x, z) \in \Omega^{(k)}$, the equation (26) on $w_1^{(k)}$ is a first order linear Cauchy problem of the form $w'(t) + a(t)w(t) = -b(t)$ with $a(t) = \partial_2 g(u_0(t, x), w_0(t, x))$ and $b(t) = \partial_1 g(u_0(t, x), w_0(t, x)) u_1^{(k)}(t, x, z)$ and with $w(0) = 0$ because $w_1^{(k)}(0, x, z) = 0$ (eq. (17)). Its solution is computed explicitly: $w(t) = -\int_0^t b(s) \exp\left(-\int_s^t a(\tau) d\tau\right) ds$. We note that the function $a(t)$ is independent of z and the functions $z \mapsto b(t)$ ($k = 1, 2$) are C^∞ (polynomial) functions for all $t \geq 0$ and a.e. $x \in \omega$. As a consequence, the functions $z \mapsto w_1^{(k)}(t, x, z)$ are C^∞ for all $t \geq 0$ and a.e. $x \in \omega$ (in fact, they are also 2nd degree polynomials). Furthermore, the function w_1 is continuous through the interface Σ , meaning that $w_1^{(1)}(t, x, 0) = w_1^{(2)}(t, x, 0)$ for all $t \geq 0$ and a.e. $x \in \omega$ (because it is true for $u_1^{(k)}$).

Afterwards, we integrate again equation (25) for $z \in (0, 1)$ and $z \in (-1, 0)$, add the resulting equations, use the transmission conditions (14) and (15) on $u_2^{(k)}$. We remark that

$$\frac{1}{2} \operatorname{div}_x \left(\sigma^{(1)} \nabla_x \bar{u}_1^{(1)} + \sigma^{(2)} \nabla_x \bar{u}_1^{(2)} \right) = \operatorname{div}_x \left(\sigma^m \nabla_x \bar{u}_1 + \sigma^d \nabla_x \frac{\bar{u}_1^{(1)} - \bar{u}_1^{(2)}}{2} \right),$$

recall that $\frac{\bar{u}_1^{(1)} - \bar{u}_1^{(2)}}{2} = \frac{1}{3} \frac{b}{\sigma_3^h}$, and finally obtain the following equations for (\bar{u}_1, \bar{w}_1) :

$$\alpha \left(\partial_t \bar{u}_1 + \beta \nabla f(u_0, w_0) \cdot (\bar{u}_1, \bar{w}_1) \right) = \operatorname{div}_x \left(\sigma^m \nabla_x \bar{u}_1 \right) + \operatorname{div}_x \left(\frac{1}{3\sigma_3^h} \sigma^d \nabla_x b \right), \quad (27)$$

$$\partial_t \bar{w}_1 + \nabla g(u_0, w_0) \cdot (\bar{u}_1, \bar{w}_1) = 0 \quad (28)$$

with the boundary condition $\sigma^m \nabla_x \bar{u}_1 \cdot n + \frac{1}{2\sigma_3^h} \sigma^d \nabla_x b \cdot n = 0$ on $\partial\omega$ and for $t > 0$, and the initial conditions $\bar{u}_1(0, x) = 0$ and $\bar{w}_1(0, x) = 0$ for a.e. $x \in \omega$.

4.2 Definition of the first order solution and associated asymptotic problem

Consider some data (u^0, w^0) defined for $x \in \omega$ and the solutions (u_0, w_0) and (\bar{u}_1, \bar{w}_1) to the bi-dimensional systems of equations (22), (23), and (27), (28), respectively, for $t > 0$ and $x \in \omega$, and with the boundary conditions

$$\sigma^m \nabla_x u_0 \cdot n = 0, \quad \sigma^m \nabla_x \bar{u}_1 \cdot n + \frac{1}{3\sigma_3^h} \sigma^d \nabla_x b \cdot n = 0,$$

and the initial condition

$$u_0(0, x) = u^0(x), \quad w_0(0, x) = w^0(x), \quad \text{and} \quad \bar{u}_1(0, x) = 0, \quad \bar{w}_1(0, x) = 0,$$

for a.e. $x \in \omega$. In equation (27) and (28), the functions u_0 and w_0 are the solutions to (22), (23), and the function b is defined on $(0, +\infty) \times \omega$ by $b = \operatorname{div}_x (\sigma^d \nabla_x u_0)$. Afterwards, we define the three-dimensional functions $u_1^{(k)}$ and $w_1^{(k)}$ on $(0, +\infty) \times \Omega^{(k)}$ for $k = 1, 2$ as follows: the function $u_1^{(k)}$ is explicitly given by

$$u_1^{(k)} = \frac{b}{\sigma_3^{(k)}} z \left(1 - \frac{|z|}{2} \right) + c, \quad \text{with} \quad c = \bar{u}_1 - \frac{1}{6} b \frac{\sigma_3^{(2)} - \sigma_3^{(1)}}{\sigma_3^{(1)} \sigma_3^{(2)}} \quad (29)$$

(from eq. (24)) and the function $w_1^{(k)}$ is the solution to the system of equations (26) for $k = 1, 2$ that also reads:

$$w_1^{(k)}(t, x, z) = - \int_0^t \partial_1 g(u_0(s, x), w_0(s, x)) u_1^{(k)}(s, x, z) \exp\left(- \int_s^t \partial_2 g(u_0(\tau, x), w_0(\tau, x)) d\tau\right) ds. \quad (30)$$

Remark 3 (Averages of $u_1^{(k)}, w_1^{(k)}$). Given the solutions \bar{u}_1 and \bar{w}_1 to (27) and (28), consider the functions $u_1^{(k)}, w_1^{(k)}$ defined by the equalities (29) and (30) above. Some straightforward computations show that, conversely, the averages in the thickness of $u_1^{(k)}$ and $w_1^{(k)}$ are exactly $\bar{u}_1 = c + \frac{1}{6}b \frac{\sigma_3^{(2)} - \sigma_3^{(1)}}{\sigma_3^{(2)} \sigma_3^{(1)}}$ and \bar{w}_1 , the given solutions to the equations (27) and (28).

While (u_0, w_0) is the solution of order 0, we define the first order approximate solution $\tilde{u}_\varepsilon^{(k)}$ and $\tilde{w}_\varepsilon^{(k)}$ on $(0, +\infty) \times \Omega^{(k)}$ by:

$$\tilde{u}_\varepsilon^{(k)}(t, x, z) = u_0(t, x) + \varepsilon^2 u_1^{(k)}(t, x, z), \quad \tilde{w}_\varepsilon^{(k)}(t, x, z) = w_0(t, x) + \varepsilon^2 w_1^{(k)}(t, x, z),$$

and the corresponding errors with respect to the complete three-dimensional solution, $e_\varepsilon^{(k)}$ and $f_\varepsilon^{(k)}$, by

$$e_\varepsilon^{(k)} := u_\varepsilon^{(k)} - \tilde{u}_\varepsilon^{(k)}, \quad f_\varepsilon^{(k)} := w_\varepsilon^{(k)} - \tilde{w}_\varepsilon^{(k)}. \quad (31)$$

4.3 Error estimate for the one-layer model

We consider some bounded initial data $u^0(x) \in L^\infty(\omega)$, $w^0(x) \in [L^\infty(\omega)]^m$, we define the functions $u_\varepsilon^{(k)}$ and $w_\varepsilon^{(k)}$ solutions to the original three-dimensional system of equations (12) and (13) with the boundary and interface conditions (14) to (16) and the initial condition $u_\varepsilon^{(k)}(0, x, z) = u^0(x)$ and $w_\varepsilon^{(k)}(0, x, z) = w^0(x)$ for $(x, z) \in \Omega^{(k)}$, $k = 1, 2$.

In Theorem 1 below, we prove that the errors $e_\varepsilon^{(k)} := u_\varepsilon^{(k)} - \tilde{u}_\varepsilon^{(k)}$ and $f_\varepsilon^{(k)} := w_\varepsilon^{(k)} - \tilde{w}_\varepsilon^{(k)}$ are bounded by ε^3 in $L^2(\Omega^{(k)})$ for all time $t > 0$, and that $e_\varepsilon^{(k)}$ is also bounded by ε^3 in $L^2(0, t; H^1(\Omega^{(k)}))$ also for all time $t > 0$.

Theorem 1 (Error estimates for the one-layer model) Assume that the functions f and g are $C^2(\mathbb{R} \times \mathbb{R}^m)$; and that the solutions (u_0, w_0) and $(u_1^{(k)}, w_1^{(k)})$ are bounded in $\mathbb{R} \times \mathbb{R}^m$, uniformly in time; and that the solutions $(u_\varepsilon^{(k)}, w_\varepsilon^{(k)})_{\varepsilon > 0}$ are bounded uniformly with respect to ε and time $t > 0$. Specifically, we require that there exists $M > 0$ such that, for all $t > 0$ and $(x, z) \in \Omega^{(k)}$ ($k = 1, 2$),

$$|(u_0(t, x), w_0(t, x))| \leq M, \quad \left| \left(u_1^{(k)}(t, x, z), w_1^{(k)}(t, x, z) \right) \right| \leq M,$$

and for all $\varepsilon > 0$, for all $t > 0$ and $(x, z) \in \Omega^{(k)}$ ($k = 1, 2$),

$$\left| \left(u_\varepsilon^{(k)}(t, x, z), w_\varepsilon^{(k)}(t, x, z) \right) \right| \leq 2M.$$

We now define the functions $\Psi^{(1)}(t, x, z) = - \int_z^1 \phi^{(1)}(t, x, \zeta) d\zeta$ and $\Psi^{(2)}(t, x, z) = \int_{-1}^z \phi^{(2)}(t, x, \zeta) d\zeta$ where the functions $\phi^{(k)}$ are given by equation (36) below. We assume that $d_1(s) := \bar{\sigma} \sum_{k=1,2} \|\Psi^{(k)}(s)\|_{L^2(\Omega^{(k)})}^2 ds$ belongs to $L_{loc}^1(\mathbb{R}^+)$.

Then, we have the following estimates, for all $0 < \varepsilon \leq 1$, for all $t > 0$, and for $k = 1, 2$,

$$\left\| e_\varepsilon^{(k)}(t) \right\|_{L^2(\Omega^{(k)})} \leq \varepsilon^3 k_0(t) \exp\left(\frac{c_0}{2}t\right), \quad (32)$$

$$\left\| f_\varepsilon^{(k)}(t) \right\|_{(L^2(\Omega^{(k)}))^m} \leq \varepsilon^3 k_0(t) \exp\left(\frac{c_0}{2}t\right), \quad (33)$$

$$\left\| \nabla_x e_\varepsilon^{(k)} \right\|_{L^2(0,t;L^2(\Omega^{(k)}))} \leq \varepsilon^3 k_1(t) \exp\left(\frac{c_0}{2}t\right), \quad (34)$$

$$\left\| \partial_z e_\varepsilon^{(k)} \right\|_{L^2(0,t;L^2(\Omega^{(k)}))} \leq \sqrt{2}\varepsilon^4 k_1(t) \exp\left(\frac{c_0}{2}t\right), \quad (35)$$

with $k_0(t) = \frac{1}{\sqrt{\alpha}} \left(\frac{d_0}{c_0} + \int_0^t d_1(s) ds \right)^{1/2}$ and $k_1(t) = \left(\frac{d_0}{2\sigma c_0} (1 + c_0 t) + \frac{1}{\sigma} \int_0^t d_1(s) ds \right)^{1/2}$ and where $c_0 = 2\Lambda_0 + \frac{1}{2}\Lambda_1$ and $d_0 = \alpha\Lambda_1 M^4 |\omega|$. The constant Λ_0 and Λ_1 are the maximum norm of the gradient and Hessian of the function $(u, w) \mapsto (\beta f(u, w), g(u, w))$ in the compact set $\{(u, w) : |(u, w)| \leq 2M\} \subset \mathbb{R} \times \mathbb{R}^m$.

Along the proofs of Theorems 1, 2, and 3, we will need the following technical lemmas.

Lemma 1 Consider a function $h : u \in \mathbb{R}^p \mapsto h(u) \in \mathbb{R}^q$ of class C^2 in \mathbb{R}^p . For any u_0 and u in \mathbb{R}^p , we define $I_h(u_0, u) := h(u) - h(u_0) - \nabla h(u_0) \cdot (u - u_0) = \int_0^1 (1-t) \nabla^2 h(tu + (1-t)u_0) (u - u_0) \cdot (u - u_0) dt$, the integral remainder in the Taylor expansion. We have

$$|u_0| \leq M \text{ and } |u| \leq M \Rightarrow |I_h(u_0, u)| \leq \frac{1}{2} \sup_{|u| \leq M} |\nabla^2 h(u)| |u - u_0|^2$$

where $\nabla^2 h$ is the Hessian matrix of h .

Lemma 2 Consider a function $u : z \in [a, b] \mapsto u(z) \in \mathbb{R}$ of class C^1 in $[a, b]$ with $b - a = 1$.

$$\forall z \in [a, b], \quad |\bar{u} - u(z)| \leq \int_a^b |u'(t)| dt$$

where $\bar{\cdot}$ denotes the mean on $[a, b]$.

Lemma 3 (Gronwall) Suppose that $y(t) \geq 0$ is a C^1 function of $t > 0$, and $h(t) \geq 0$, $d_1(t) \geq 0$ are functions in $L_{loc}^1((0, +\infty))$. Consider some constants $c_0 > 0$ and $d_0 > 0$. For all $\varepsilon > 0$, if

$$y'(t) + h(t) \leq c_0 y(t) + \varepsilon^6 (d_0 + d_1(t)),$$

for all $t > 0$, and $y(0) = 0$, then

$$y(t) \leq \varepsilon^6 \left(\frac{d_0}{c_0} + \int_0^t d_1(s) ds \right) \exp(c_0 t),$$

$$\int_0^t h(s) ds \leq \varepsilon^6 \left(\frac{d_0}{c_0} (1 + c_0 t) + 2 \int_0^t d_1(s) ds \right) \exp(c_0 t).$$

Proof:

Let us prove Lemmas 1 to 3. Lemmas 1 and 2 are straightforward derivations of Taylor expansions with integral remainders. Lemma 3 is a direct consequence of the usual inequality of Gronwall $y(t) \leq \exp(c_0 t) y(0) + \int_0^t \varepsilon^6 (d_0 + d_1(s)) \exp(c_0(t-s)) ds$. We obtain the first inequality because $y(0) = 0$ and $\int_0^t \exp(c_0(t-s)) ds \leq \frac{1}{c_0} \exp(c_0 t)$ and $\exp(c_0(t-s)) \leq \exp(c_0 t)$, for $0 \leq s \leq t$. Hence, we integrate this inequality to obtain $\int_0^t y(s) ds \leq \varepsilon^6 \left(\frac{d_0}{c_0} + \int_0^t d_1(s) ds \right) \frac{1}{c_0} \exp(c_0 t)$. The final result is a direct consequence of the integrated inequality: $\int_0^t h(s) ds \leq c_0 \int_0^t y(s) ds + \varepsilon^6 (d_0 t + \int_0^t d_1(s) ds)$.

□

Proof:

of Theorem 1. We define the functions $\phi^{(k)}$ on $(0, +\infty) \times \Omega^{(k)}$ for $k = 1, 2$ by

$$\sigma_3^{(k)} \phi^{(k)} = \alpha \left(\partial_t u_1^{(k)} + \beta \nabla f(u_0, w_0) \cdot \left(u_1^{(k)}, w_1^{(k)} \right) \right) - \operatorname{div}_x \left(\sigma^{(k)} \nabla_x u_1^{(k)} \right). \quad (36)$$

The functions $\phi^{(k)}$ play the role of the functions $\partial_{zz} u_2^{(k)}$ in the formal expansion of the previous section. The functions $\psi^{(1)}(t, x, z) = -\int_z^1 \phi^{(1)}(t, x, \zeta) d\zeta$ and $\psi^{(2)}(t, x, z) = \int_{-1}^z \phi^{(2)}(t, x, \zeta) d\zeta$ are such that $\psi^{(1)}(\cdot, 1) = 0$, $\psi^{(2)}(\cdot, -1) = 0$, and $\partial_z \psi^{(k)} = \phi^{(k)}$ for $k = 1, 2$. We average the equation (36) in the whole thickness; use the result from remark 3 and the tricks used to establish equation (27) to prove that, for all $t > 0$ and a.e. $x \in \omega$,

$$\begin{aligned} & \frac{1}{2} \left(-\sigma_3^{(1)} \psi^{(1)}(\cdot, 0) + \sigma_3^{(2)} \psi^{(2)}(\cdot, 0) \right) \\ &= \alpha \left(\partial_t \bar{u}_1 + \beta \nabla f(u_0, w_0) \cdot (\bar{u}_1, \bar{w}_1) \right) - \operatorname{div}_x \left(\sigma^m \nabla_x \bar{u}_1 \right) - \operatorname{div}_x \left(\frac{1}{3\sigma_3^h} \sigma^d \nabla_x b \right) = 0 \end{aligned}$$

because \bar{u}_1 and \bar{w}_1 are solutions to the system (27), (28). It shows that $\sigma_3^{(1)} \psi^{(1)}(\cdot, 0) = \sigma_3^{(2)} \psi^{(2)}(\cdot, 0)$, that is the transmission condition (16).

A linear combination of the equations that define $u_\varepsilon^{(k)}$, $w_\varepsilon^{(k)}$, u_0 , w_0 and $u_1^{(k)}$, $w_1^{(k)}$, and the definition of $\psi^{(k)}$ immediately shows that

$$\begin{aligned} & \alpha \left(\partial_t \left(u_\varepsilon^{(k)} - u_0 - \varepsilon^2 u_1^{(k)} \right) \right. \\ & \quad \left. + \beta \left(f(u_\varepsilon^{(k)}, w_\varepsilon^{(k)}) - f(u_0, w_0) - \varepsilon^2 \nabla f(u_0, w_0) \cdot \left(u_1^{(k)}, w_1^{(k)} \right) \right) \right) \\ &= \operatorname{div}_x \left(\sigma^{(k)} \nabla_x u_\varepsilon^{(k)} - \sigma^m \nabla_x u_0 - \varepsilon^2 \sigma^{(k)} \nabla_x u_1^{(k)} \right) + \frac{\sigma_3^{(k)}}{\varepsilon^2} \partial_{zz} u_\varepsilon^{(k)} - \varepsilon^2 \sigma_3^{(k)} \partial_z \psi^{(k)}, \end{aligned}$$

and (see also remark 3)

$$\begin{aligned} & \partial_t \left(w_\varepsilon^{(k)} - w_0 - \varepsilon^2 w_1^{(k)} \right) \\ & \quad + \left(g(u_\varepsilon^{(k)}, w_\varepsilon^{(k)}) - g(u_0, w_0) - \varepsilon^2 \nabla g(u_0, w_0) \cdot \left(u_1^{(k)}, w_1^{(k)} \right) \right) = 0. \end{aligned}$$

Now, remark that

$$\begin{aligned} & \operatorname{div}_x \left(\sigma^{(k)} \nabla_x u_\varepsilon^{(k)} - \sigma^m \nabla_x u_0 - \varepsilon^2 \sigma^{(k)} \nabla_x u_1^{(k)} \right) \\ &= \operatorname{div}_x \left(\sigma^{(k)} \nabla_x \left(u_\varepsilon^{(k)} - u_0 - \varepsilon^2 u_1^{(k)} \right) \right) + \operatorname{div}_x \left((\sigma^{(k)} - \sigma^m) \nabla_x u_0 \right) \\ & \quad = \operatorname{div}_x \left(\sigma^{(k)} \nabla_x e_\varepsilon^{(k)} \right) - \sigma_3^{(k)} \partial_{zz} u_1^{(k)} \end{aligned}$$

because we have $\sigma^{(k)} - \sigma^m = \frac{\sigma^{(1)} - \sigma^{(2)}}{2} = \sigma^d$ if $k = 1$ and $\sigma^{(k)} - \sigma^m = \frac{\sigma^{(2)} - \sigma^{(1)}}{2} = -\sigma^d$ if $k = 2$, so that

$$\operatorname{div}_x \left((\sigma^{(k)} - \sigma^m) \nabla_x u_0 \right) = \begin{cases} b = -\sigma_3^{(1)} \partial_{zz} u_1^{(1)} & \text{if } k = 1, \\ -b = -\sigma_3^{(2)} \partial_{zz} u_1^{(2)} & \text{if } k = 2. \end{cases}$$

Remark at last that $\partial_{zz}u_\varepsilon^{(k)} - \varepsilon^2\partial_{zz}u_1^{(k)} = \partial_{zz}\left(u_\varepsilon^{(k)} - u_0 - \varepsilon^2u_1^{(k)}\right) = \partial_{zz}e_\varepsilon^{(k)}$ because $\partial_{zz}u_0 = 0$. We obtain the following equations on the errors $e_\varepsilon^{(k)}$ and $f_\varepsilon^{(k)}$:

$$\alpha\left(\partial_t e_\varepsilon^{(k)} + \beta E_\varepsilon^{(k)}(f)\right) = \operatorname{div}_x\left(\sigma^{(k)}\nabla_x e_\varepsilon^{(k)}\right) + \frac{\sigma_3^{(k)}}{\varepsilon^2}\partial_{zz}e_\varepsilon^{(k)} - \varepsilon^2\sigma_3^{(k)}\partial_z\psi^{(k)}, \quad (37)$$

$$\partial_t f_\varepsilon^{(k)} + E_\varepsilon^{(k)}(g) = 0, \quad (38)$$

where $E_\varepsilon^{(k)}(f) = f(u_\varepsilon^{(k)}, w_\varepsilon^{(k)}) - f(u_0, w_0) - \varepsilon^2\nabla f(u_0, w_0) \cdot (u_1^{(k)}, w_1^{(k)})$ and $E_\varepsilon^{(k)}(g) = g(u_\varepsilon^{(k)}, w_\varepsilon^{(k)}) - g(u_0, w_0) - \varepsilon^2\nabla g(u_0, w_0) \cdot (u_1^{(k)}, w_1^{(k)})$. For $k = 1, 2$, we multiply the first equation by $e_\varepsilon^{(k)}$ and the second by $\alpha f_\varepsilon^{(k)}$, integrate on $\Omega^{(k)}$ and add the resulting equations in order to obtain the following energy estimate:

$$\begin{aligned} \frac{1}{2}\frac{d}{dt}y(t) + \sum_{k=1,2}\int_{\Omega^{(k)}}\left(\underline{\sigma}\left|\nabla_x e_\varepsilon^{(k)}\right|^2 + \frac{\sigma_3^{(k)}}{\varepsilon^2}\left|\partial_{zz}e_\varepsilon^{(k)}\right|^2\right) dzdx \\ \leq \sum_{k=1,2}\int_{\Omega^{(k)}}\alpha\left|\beta E_\varepsilon^{(k)}(f)e_\varepsilon^{(k)} + E_\varepsilon^{(k)}(g) \cdot f_\varepsilon^{(k)}\right| dzdx \\ + \sum_{k=1,2}\int_{\Omega^{(k)}}\sigma_3^{(k)}\left|\varepsilon^2\psi^{(k)}\partial_z e_\varepsilon^{(k)}\right| dzdx, \end{aligned}$$

where $y(t) = \alpha\sum_{k=1,2}\left(\|e_\varepsilon^{(k)}\|_{L^2(\Omega^{(k)})}^2 + \|f_\varepsilon^{(k)}\|_{L^2(\Omega^{(k)})}^2\right)$ is the total L^2 norm of the error. Remark that $e_\varepsilon^{(k)}$ and $\psi^{(k)}$ verify the boundary and transmission conditions (14) to (16). Consequently, the boundary terms vanish and the interface terms cancel each other in the energy estimate. Specifically, we have that $\sigma_\varepsilon^{(k)}\nabla_x e_\varepsilon^{(k)} \cdot n = 0$ for $x \in \partial\omega$ and $z \in (0, 1)$ (for $k = 1$) or $z \in (-1, 0)$ (for $k = 2$); $\sigma_3^{(k)}\partial_z e_\varepsilon^{(k)} = 0$ and $\psi^{(k)} = 0$ for $x \in \omega$ and $z = 1$ (for $k = 1$) or $z = -1$ (for $k = 2$). The terms on the interface cancel each other because $\sigma_3^{(1)}\partial_z e_\varepsilon^{(1)} = \sigma_3^{(2)}\partial_z e_\varepsilon^{(2)}$, $\sigma_3^{(1)}\psi^{(1)} = \sigma_3^{(2)}\psi^{(2)}$ and $e_\varepsilon^{(1)} = e_\varepsilon^{(2)}$ for $x \in \omega$ and $z = 0$ (just remark that u_0 is independent of z , recall the expression (24) of $u_1^{(k)}$ and the transmission condition for $u_\varepsilon^{(k)}$).

Using the inequality $\left|\varepsilon^2\psi^{(k)}\partial_z e_\varepsilon^{(k)}\right| \leq \frac{\varepsilon^6|\psi^{(k)}|^2}{2} + \frac{|\partial_z e_\varepsilon^{(k)}|^2}{2\varepsilon^2}$, we obtain the inequality

$$\begin{aligned} \frac{1}{2}\frac{d}{dt}y(t) + \underline{\sigma}\sum_{k=1,2}\int_{\Omega^{(k)}}\left(\left|\nabla_x e_\varepsilon^{(k)}\right|^2 + \frac{1}{2\varepsilon^2}\left|\partial_z e_\varepsilon^{(k)}\right|^2\right) dzdx \\ \leq \alpha\sum_{k=1,2}\int_{\Omega^{(k)}}\left|E_\varepsilon^{(k)}(\beta f, g) \cdot (e_\varepsilon^{(k)}, f_\varepsilon^{(k)})\right| dzdx + \frac{\bar{\sigma}}{2}\varepsilon^6\sum_{k=1,2}\int_{\Omega^{(k)}}\left|\psi^{(k)}\right|^2 dzdx, \end{aligned}$$

where $E_\varepsilon^{(k)}(\beta f, g) = (\beta E_\varepsilon^{(k)}(f), E_\varepsilon^{(k)}(g))$. We now define the function $\mathbf{f}: (u, w) \in \mathbb{R} \times \mathbb{R}^m \mapsto (\beta f(u, w), g(u, w)) \in \mathbb{R} \times \mathbb{R}^m$, and use Lemma 1, so that, for $k = 1, 2$,

$$\begin{aligned} \left|E_\varepsilon^{(k)}(\beta f, g)\right| &= \left|\mathbf{f}(u_\varepsilon^{(k)}, w_\varepsilon^{(k)}) - \mathbf{f}(u_0, w_0) - \varepsilon^2\nabla\mathbf{f}(u_0, w_0) \cdot (u_1^{(k)}, w_1^{(k)})\right| \\ &\leq \left|\mathbf{f}(u_\varepsilon^{(k)}, w_\varepsilon^{(k)}) - \mathbf{f}(\tilde{u}_\varepsilon^{(k)}, \tilde{w}_\varepsilon^{(k)})\right| + \left|I_{\mathbf{f}}(u_0, w_0; \tilde{u}_\varepsilon^{(k)}, \tilde{w}_\varepsilon^{(k)})\right| \\ &\leq \Lambda_0\left|(e_\varepsilon^{(k)}, f_\varepsilon^{(k)})\right| + \frac{1}{2}\Lambda_1\varepsilon^4\left|(u_1^{(k)}, w_1^{(k)})\right|^2 \leq \Lambda_0\left|(e_\varepsilon^{(k)}, f_\varepsilon^{(k)})\right| + \frac{1}{2}\Lambda_1\varepsilon^4M^2 \quad (39) \end{aligned}$$

where $\Lambda_0 = \sup_{|(u,v)| \leq 2M} |\nabla\mathbf{f}(u,v)|$, $\Lambda_1 = \sup_{|(u,v)| \leq M} |\nabla^2\mathbf{f}(u,v)|$ and $I_{\mathbf{f}}$ is defined in Lemma 1. Here, we have used the fact that $\left|(\tilde{u}_\varepsilon^{(k)}, \tilde{w}_\varepsilon^{(k)})\right| \leq M(1 + \varepsilon^2) \leq 2M$ for $\varepsilon \leq 1$, because of the assumptions on

$(u_\varepsilon^{(k)}, w_\varepsilon^{(k)})$, (u_0, w_0) and $(u_1^{(k)}, w_1^{(k)})$. Now, we can write the last estimate:

$$\begin{aligned} & \alpha \sum_{k=1,2} \int_{\Omega^{(k)}} \left| E_\varepsilon^{(k)}(\beta f, g) \cdot (e_\varepsilon^{(k)}, f_\varepsilon^{(k)}) \right| dz dx \\ & \leq \alpha \sum_{k=1,2} \int_{\Omega^{(k)}} \Lambda_0 \left| (e_\varepsilon^{(k)}, f_\varepsilon^{(k)}) \right|^2 dx dz + \alpha \sum_{k=1,2} \int_{\Omega^{(k)}} \frac{1}{2} \Lambda_1 \varepsilon^4 \left| (e_\varepsilon^{(k)}, f_\varepsilon^{(k)}) \right| M^2 dx dz \\ & \leq \left(\Lambda_0 + \frac{1}{4} \Lambda_1 \right) y(t) + \frac{1}{2} \alpha \Lambda_1 \varepsilon^8 M^4 |\omega| \end{aligned}$$

with the inequality of Young $\varepsilon^4 \left| (e_\varepsilon^{(k)}, f_\varepsilon^{(k)}) \right| M^2 \leq \frac{1}{2} \left(\left| (e_\varepsilon^{(k)}, f_\varepsilon^{(k)}) \right|^2 + \varepsilon^8 M^4 \right)$ and because $\sum_{k=1,2} |\Omega^{(k)}| = 2|\omega|$. The final energy estimate reads:

$$\begin{aligned} & \frac{1}{2} \frac{d}{dt} y(t) + \underline{\sigma} \sum_{k=1,2} \int_{\Omega^{(k)}} \left(\left| \nabla_x e_\varepsilon^{(k)} \right|^2 + \frac{1}{2\varepsilon^2} \left| \partial_z e_\varepsilon^{(k)} \right|^2 \right) dz dx \\ & \leq \left(\Lambda_0 + \frac{1}{4} \Lambda_1 \right) y(t) + \frac{1}{2} \alpha \Lambda_1 \varepsilon^8 M^4 |\omega| + \frac{\bar{\sigma}}{2} \varepsilon^6 \sum_{k=1,2} \|\psi^{(k)}(t)\|_{L^2(\Omega^{(k)})}^2. \end{aligned}$$

We assume that $\varepsilon \leq 1$, so that $\varepsilon^8 \leq \varepsilon^6$ and simplify the inequality by noting $c_0 = 2\Lambda_0 + \frac{1}{2}\Lambda_1$, $d_0 = \alpha\Lambda_1 M^4 |\omega|$ and $d_1(t) = \bar{\sigma} \sum_{k=1,2} \|\psi^{(k)}(t)\|_{L^2(\Omega^{(k)})}^2$. Hence, we have the inequality $y'(t) + h(t) \leq c_0 y(t) + (d_0 + d_1(t)) \varepsilon^6$ for any $t \geq 0$ (and for $h(t) = \underline{\sigma} \sum_{k=1,2} \int_{\Omega^{(k)}} \left(\left| \nabla_x e_\varepsilon^{(k)} \right|^2 + \frac{1}{2\varepsilon^2} \left| \partial_z e_\varepsilon^{(k)} \right|^2 \right) dz dx$), and can apply Lemma 3 to complete the proof. \square

Remark 4 An asymptotic expansion of the initial data could be carried out without additional difficulties, if the initial data were not constant along z . The final error estimate is of order ε^3 , whereas a continuation of the formal study in the beginning of the section 4.1 would show that the coefficient of order ε^3 vanishes, and that the convergence order is of order ε^4 . This is a usual fact when estimating the error of the asymptotic expansion by a L^2 energy method see Lions [1973].

Theorem 2 (Additional error estimates) Under the assumptions of Theorem 1, let us assume additionally that for all $t > 0$ and a.e. $x \in \omega$, the functions $z \mapsto u_1^{(k)}(t, x, z)$ and $z \mapsto w_1^{(k)}(t, x, z)$ belong to $H^2(0, 1)$ if $k = 1$ and $H^2(-1, 0)$ if $k = 2$, and for all for all $t > 0$ and a.e. $(x, z) \in \Omega^{(k)}$,

$$\left| \left(\partial_z u_1^{(k)}(t, x, z), \partial_z w_1^{(k)}(t, x, z) \right) \right| \leq M, \quad \left| \left(\partial_z^3 u_\varepsilon^{(k)}(t, x, z), \partial_z w_\varepsilon^{(k)}(t, x, z) \right) \right| \leq 2M,$$

with the bound M from Theorem 1. Assume that $\sum_{k=1,2} \|\partial_z \psi^{(k)}(s)\|_{L^2(\Omega^{(k)})}^2$ belongs to $L^1_{loc}(\mathbb{R}^+)$. Then, we have the following estimates, for all $0 < \varepsilon \leq 1$, for all $t > 0$, and for $k = 1, 2$,

$$\left\| \partial_z e_\varepsilon^{(k)}(t) \right\|_{L^2(\Omega^{(k)})} \leq \varepsilon^3 k_2(t) \exp\left(\frac{c_1}{2} t\right), \quad (40)$$

$$\left\| \partial_z f_\varepsilon^{(k)}(t) \right\|_{(L^2(\Omega^{(k)}))^m} \leq \varepsilon^3 k_2(t) \exp\left(\frac{c_1}{2} t\right), \quad (41)$$

$$\left\| \nabla_x \partial_z e_\varepsilon^{(k)} \right\|_{L^2(0,t;L^2(\Omega^{(k)}))} \leq \varepsilon^3 k_3(t) \exp\left(\frac{c_1}{2} t\right), \quad (42)$$

$$\left\| \partial_{zz} e_\varepsilon^{(k)}(t) \right\|_{L^2(0,t;L^2(\Omega^{(k)}))} \leq \sqrt{2} \varepsilon^4 k_3(t) \exp\left(\frac{c_1}{2} t\right), \quad (43)$$

with $k_2(t) = \frac{1}{\sqrt{\alpha\bar{\sigma}}} \left(\frac{d_2}{c_1} + \int_0^t d_3(s) ds \right)^{1/2}$, $k_3(t) = \frac{1}{\bar{\sigma}\sqrt{2}} \left(\frac{d_2}{c_1} (1 + c_1 t) + 2 \int_0^t d_3(s) ds \right)^{1/2}$, and where $c_1 = 2(\Lambda_0 + \Lambda_1)$, $d_2 = 2\alpha\bar{\sigma}\Lambda_1 M^4 |\omega| = 2\bar{\sigma}d_0$, and

$$d_3(t) = \alpha\Lambda_1\bar{\sigma}M^2 k_0(t)^2 \exp(c_0 t) + \bar{\sigma} \sum_{k=1,2} \|\partial_z \psi^{(k)}(t)\|_{L^2(\Omega^{(k)})}^2.$$

We use Lemma 4 below, which proof is postponed to the appendix.

Lemma 4 For all $t > 0$, and a.e. $x \in \omega$, the functions $w_\varepsilon^{(k)}$ verify exactly the transmission condition (16):

$$w_\varepsilon^{(1)}(t, x, 0) = w_\varepsilon^{(2)}(t, x, 0), \quad \text{and} \quad \sigma_3^{(1)} \partial_z w_\varepsilon^{(1)}(t, x, 0) = \sigma_3^{(2)} \partial_z w_\varepsilon^{(2)}(t, x, 0).$$

Proof:

of Theorem 2. We test the equations (37) and (38) on the errors against the functions $-\sigma_3^{(k)} \partial_{zz} e_\varepsilon^{(k)}$ and $-\alpha\sigma_3^{(k)} \partial_{zz} f_\varepsilon^{(k)}$. In order to complete the integration by parts in z , note that

$$-\sum_{k=1,2} \int_{\Omega^{(k)}} \sigma_3^{(k)} \partial_{zz} e_\varepsilon^{(k)} \partial_t e_\varepsilon^{(k)} dx dz = \frac{1}{2} \frac{d}{dt} \sum_{k=1,2} \int_{\Omega^{(k)}} \sigma_3^{(k)} \left| \partial_z e_\varepsilon^{(k)} \right|^2 dx dz,$$

and after integration by parts in x and z ,

$$\begin{aligned} -\sum_{k=1,2} \int_{\Omega^{(k)}} \operatorname{div}_x \left(\sigma^{(k)} \nabla_x e_\varepsilon^{(k)} \right) \sigma_3^{(k)} \partial_{zz} e_\varepsilon^{(k)} dz dx \\ = -\sum_{k=1,2} \int_{\Omega^{(k)}} \left(\sigma^{(k)} \nabla_x \partial_z e_\varepsilon^{(k)} \right) \cdot \left(\sigma_3^{(k)} \nabla_x \partial_z e_\varepsilon^{(k)} \right) dz dx, \end{aligned}$$

both because $e_\varepsilon^{(k)}$ ($k = 1, 2$) verify the boundary and transmission conditions (14) to (16), so that we finally have:

$$\begin{aligned} \frac{1}{2} \frac{d}{dt} y(t) + \sum_{k=1,2} \int_{\Omega^{(k)}} \left(\bar{\sigma}^2 \left| \nabla_x \partial_z e_\varepsilon^{(k)} \right|^2 + \frac{\sigma_3^{(k)2}}{\varepsilon^2} \left| \partial_{zz} e_\varepsilon^{(k)} \right|^2 \right) dz dx \\ \leq \alpha \sum_{k=1,2} \int_{\Omega^{(k)}} \sigma_3^{(k)} E_\varepsilon^{(k)}(\beta f, g) \cdot \left(\partial_{zz} e_\varepsilon^{(k)}, \partial_{zz} f_\varepsilon^{(k)} \right) dx dz \\ + \varepsilon^2 \sum_{k=1,2} \int_{\Omega^{(k)}} \sigma_3^{(k)2} \partial_z \psi^{(k)} \partial_{zz} e_\varepsilon^{(k)} dx dz \end{aligned}$$

with now $y(t) = \alpha \sum_{k=1,2} \sigma_3^{(k)} \left(\|\partial_z e_\varepsilon^{(k)}\|_{L^2(\Omega^{(k)})}^2 + \|\partial_z f_\varepsilon^{(k)}\|_{(L^2(\Omega^{(k)}))^m}^2 \right)$. After integration by parts in the first term of the right-hand side of this inequality using Lemma 4, and the inequality of Young for the second one, we find that:

$$\begin{aligned} \frac{1}{2} \frac{d}{dt} y(t) + \bar{\sigma}^2 \sum_{k=1,2} \int_{\Omega^{(k)}} \left(\left| \nabla_x \partial_z e_\varepsilon^{(k)} \right|^2 + \frac{1}{2\varepsilon^2} \left| \partial_{zz} e_\varepsilon^{(k)} \right|^2 \right) dz dx \\ \leq \alpha \sum_{k=1,2} \int_{\Omega^{(k)}} \sigma_3^{(k)} \left| \partial_z E_\varepsilon^{(k)}(\beta f, g) \cdot \left(\partial_z e_\varepsilon^{(k)}, \partial_z f_\varepsilon^{(k)} \right) \right| dx dz \\ + \frac{\bar{\sigma}^2}{2} \varepsilon^6 \sum_{k=1,2} \int_{\Omega^{(k)}} \left| \partial_z \psi^{(k)} \right|^2 dx dz. \end{aligned}$$

Afterwards, we remark that

$$\begin{aligned} \partial_z \left(E_\varepsilon^{(k)}(\beta f, g) \right) &= \nabla \mathbf{f}(u_\varepsilon^{(k)}, w_\varepsilon^{(k)}) \cdot \left(\partial_z u_\varepsilon^{(k)}, \partial_z w_\varepsilon^{(k)} \right) - \\ &\quad \varepsilon^2 \nabla \mathbf{f}(u_0, w_0) \cdot \left(\partial_z u_1^{(k)}, \partial_z w_1^{(k)} \right), \end{aligned}$$

and that $\left(\partial_z u_\varepsilon^{(k)}, \partial_z w_\varepsilon^{(k)} \right) = \left(\partial_z e_\varepsilon^{(k)}, \partial_z f_\varepsilon^{(k)} \right) + \varepsilon^2 \left(\partial_z u_1^{(k)}, \partial_z w_1^{(k)} \right)$. Then

$$\begin{aligned} \left| \partial_z \left(E_\varepsilon^{(k)}(\beta f, g) \right) \right| &\leq \left| \nabla \mathbf{f}(u_\varepsilon^{(k)}, w_\varepsilon^{(k)}) \right| \left| \left(\partial_z e_\varepsilon^{(k)}, \partial_z f_\varepsilon^{(k)} \right) \right| \\ &\quad + \varepsilon^2 \left| \nabla \mathbf{f}(u_\varepsilon^{(k)}, w_\varepsilon^{(k)}) - \nabla \mathbf{f}(u_0, w_0) \right| \left| \left(\partial_z u_1^{(k)}, \partial_z w_1^{(k)} \right) \right| \\ &\leq \Lambda_0 \left| \left(\partial_z e_\varepsilon^{(k)}, \partial_z f_\varepsilon^{(k)} \right) \right| \\ &\quad + \varepsilon^2 \Lambda_1 \left| \left(\partial_z u_1^{(k)}, \partial_z w_1^{(k)} \right) \right| \left(\left| \left(e_\varepsilon^{(k)}, f_\varepsilon^{(k)} \right) \right| + \varepsilon^2 \left| \left(u_1^{(k)}, w_1^{(k)} \right) \right| \right) \end{aligned}$$

because $\left(u_\varepsilon^{(k)}, w_\varepsilon^{(k)} \right) - \left(u_0, w_0 \right) = \varepsilon^2 \left(u_1^{(k)}, w_1^{(k)} \right) + \left(e_\varepsilon^{(k)}, f_\varepsilon^{(k)} \right)$. We complete the estimate by writing:

$$\begin{aligned} &\alpha \sum_{k=1,2} \sigma_3^{(k)} \int_{\Omega^{(k)}} \left| \partial_z E_\varepsilon^{(k)}(\beta f, g) \cdot \left(\partial_z e_\varepsilon^{(k)}, \partial_z f_\varepsilon^{(k)} \right) \right| dz dx \\ &\leq \alpha \sum_{k=1,2} \int_{\Omega^{(k)}} \Lambda_0 \sigma_3^{(k)} \left| \left(\partial_z e_\varepsilon^{(k)}, \partial_z f_\varepsilon^{(k)} \right) \right|^2 dx dz \\ &\quad + \alpha \sum_{k=1,2} \int_{\Omega^{(k)}} \sigma_3^{(k)} \Lambda_1 \varepsilon^2 M \left(\left| \left(e_\varepsilon^{(k)}, f_\varepsilon^{(k)} \right) \right| + \varepsilon^2 M \right) \left| \left(\partial_z e_\varepsilon^{(k)}, \partial_z f_\varepsilon^{(k)} \right) \right| dx dz \\ &\leq \alpha \sum_{k=1,2} \int_{\Omega^{(k)}} \Lambda_0 \sigma_3^{(k)} \left| \left(\partial_z e_\varepsilon^{(k)}, \partial_z f_\varepsilon^{(k)} \right) \right|^2 dx dz \\ &\quad + \alpha \sum_{k=1,2} \int_{\Omega^{(k)}} \sigma_3^{(k)} \Lambda_1 \left(\varepsilon^2 M \left| \left(e_\varepsilon^{(k)}, f_\varepsilon^{(k)} \right) \right| \left| \left(\partial_z e_\varepsilon^{(k)}, \partial_z f_\varepsilon^{(k)} \right) \right| \right. \\ &\quad \quad \left. + \varepsilon^4 M^2 \left| \left(\partial_z e_\varepsilon^{(k)}, \partial_z f_\varepsilon^{(k)} \right) \right| \right) dx dz \\ &\leq \Lambda_0 y(t) \\ &\quad + \alpha \sum_{k=1,2} \sigma_3^{(k)} \Lambda_1 \frac{1}{2} \int_{\Omega^{(k)}} \left(\varepsilon^4 M^2 \left| \left(e_\varepsilon^{(k)}, f_\varepsilon^{(k)} \right) \right|^2 + \varepsilon^8 M^4 + 2 \left| \left(\partial_z e_\varepsilon^{(k)}, \partial_z f_\varepsilon^{(k)} \right) \right|^2 \right) dx dz \\ &\leq (\Lambda_0 + \Lambda_1) y(t) + \frac{1}{2} \Lambda_1 \bar{\sigma} M^2 \varepsilon^{10} \alpha k_0(t)^2 \exp(c_0 t) + \alpha \bar{\sigma} \Lambda_1 M^4 |\omega| \varepsilon^8, \end{aligned}$$

where we use the bounds $\left| \left(\partial_z u_1^{(k)}, \partial_z w_1^{(k)} \right) \right| \leq M$ and $\left| \left(u_1^{(k)}, w_1^{(k)} \right) \right| \leq M$, some inequalities of Young, the inequality $\alpha \sum_{k=1,2} \int_{\Omega^{(k)}} \left| \left(e_\varepsilon^{(k)}, f_\varepsilon^{(k)} \right) \right|^2 \leq \alpha k_0(t)^2 \exp(c_0 t) \varepsilon^6$ from the proof of Theorem 1, and the definition of $y(t)$. The final estimate reads:

$$\begin{aligned} \frac{d}{dt} y(t) + 2\bar{\sigma}^2 \sum_{k=1,2} \int_{\Omega^{(k)}} \left(\left| \nabla_x \partial_z e_\varepsilon^{(k)} \right|^2 + \frac{1}{2\varepsilon^2} \left| \partial_{zz} e_\varepsilon^{(k)} \right|^2 \right) dz dx \\ \leq c_1 y(t) + \varepsilon^6 (d_2 + d_3(t)) \end{aligned}$$

where the constants c_1 , d_2 , and the function $d_3(t)$ are given in the statement of Theorem 2. We conclude again with Lemma 3. \square

5 The asymptotic model with two layers

5.1 Equations on the averages through the thickness of the layers of tissue

In this section, we prove that the averages in $z \in (0, 1)$ and $z \in (-1, 0)$ for each of the two layers of the solution $(u_\varepsilon^{(k)}, w_\varepsilon^{(k)})$ verifies a system of two surface monodomain equations, linearly coupled, up to an error of order ε^3 . It is the basis for the definition of our model with two layers. Consequently, unlike in the previous case, the source function is computed from a different value of the transmembrane potential in each layer, and can have different dynamics in each layer. This is sufficient to trigger complex propagation patterns.

We integrate Equations (31) defining $e_\varepsilon^{(k)}$ and $f_\varepsilon^{(k)}$ for $z \in (0, 1)$ and $z \in (-1, 0)$, use the properties of $u_1^{(k)}$, and find that

$$\bar{u}_\varepsilon^{(k)}(t, x) = u_0(t, x) + \varepsilon^2 \left(c - (-1)^k \frac{1}{3} \frac{b}{\sigma_3^{(k)}} \right) + \bar{e}_\varepsilon^{(k)}(t, x, z).$$

We recall that $\bar{\cdot}$ denotes the integration for $z \in (0, 1)$ for $k = 1$ and $z \in (-1, 0)$ for $k = 2$. In particular, we have that

$$\frac{\bar{u}_\varepsilon^{(1)} - \bar{u}_\varepsilon^{(2)}}{2} = \varepsilon^2 \frac{1}{3} \frac{b}{\sigma_3^h} + \frac{\bar{e}_\varepsilon^{(1)} - \bar{e}_\varepsilon^{(2)}}{2}. \quad (44)$$

We derive (31) in z and obtain

$$\partial_z u_\varepsilon^{(k)} = \varepsilon^2 \partial_z u_1^{(k)} + \partial_z e_\varepsilon^{(k)} = \varepsilon^2 \frac{b}{\sigma_3^{(k)}} \left(1 + (-1)^k z \right) + \partial_z e_\varepsilon^{(k)}.$$

Now recall that $\sigma_3^{(1)} \partial_z u_\varepsilon^{(1)}(t, x, 0) = \sigma_3^{(2)} \partial_z u_\varepsilon^{(2)}(t, x, 0)$ according to the transmission condition (16), and we can define the residual

$$Su_\varepsilon(t, x) := \sigma_3^{(1)} \partial_z e_\varepsilon^{(1)}(t, x, 0) = \sigma_3^{(2)} \partial_z e_\varepsilon^{(2)}(t, x, 0) \quad (45)$$

so that

$$\sigma_3^{(1)} \partial_z u_\varepsilon^{(1)}(t, x, 0) = \sigma_3^{(2)} \partial_z u_\varepsilon^{(2)}(t, x, 0) = \varepsilon^2 b(t, x) + Su_\varepsilon(t, x).$$

Now, we are ready to integrate the monodomain equations (12) and (13) for $z \in (0, 1)$ and $z \in (-1, 0)$. This yields:

$$\begin{aligned} \alpha \left(\partial_t \bar{u}_\varepsilon^{(k)} + \beta f \left(\overline{u_\varepsilon^{(k)}, w_\varepsilon^{(k)}} \right) \right) &= \operatorname{div}_x \left(\sigma^{(k)} \nabla_x \bar{u}_\varepsilon^{(k)} \right) + (-1)^k \left(b + \frac{1}{\varepsilon^2} Su_\varepsilon \right), \\ \partial_t \bar{w}_\varepsilon^{(k)} + g \left(\overline{u_\varepsilon^{(k)}, w_\varepsilon^{(k)}} \right) &= 0. \end{aligned}$$

Like in the proof of Theorem 1, we denote by $\bar{E}_\varepsilon^{(k)}(f) := f \left(\bar{u}_\varepsilon^{(k)}, \bar{w}_\varepsilon^{(k)} \right) - \overline{f \left(u_\varepsilon^{(k)}, w_\varepsilon^{(k)} \right)}$ and $\bar{E}_\varepsilon^{(k)}(g) := g \left(\bar{u}_\varepsilon^{(k)}, \bar{w}_\varepsilon^{(k)} \right) - \overline{g \left(u_\varepsilon^{(k)}, w_\varepsilon^{(k)} \right)}$ the nonlinear errors. Afterwards, we substitute b according to Equation (44), so that the averages $(\bar{u}_\varepsilon^{(k)}, \bar{w}_\varepsilon^{(k)})$ are solutions to the monodomain system of equations, for $k = 1, 2$

$$\begin{aligned} \alpha \left(\partial_t \bar{u}_\varepsilon^{(k)} + \beta f \left(\bar{u}_\varepsilon^{(k)}, \bar{w}_\varepsilon^{(k)} \right) \right) &= \operatorname{div}_x \left(\sigma^{(k)} \nabla_x \bar{u}_\varepsilon^{(k)} \right) \\ &+ (-1)^k \left(\frac{3}{2} \sigma_3^h \frac{\bar{u}_\varepsilon^{(1)} - \bar{u}_\varepsilon^{(2)}}{\varepsilon^2} - \frac{3}{2} \sigma_3^h \frac{\bar{e}_\varepsilon^{(1)} - \bar{e}_\varepsilon^{(2)}}{\varepsilon^2} + \frac{1}{\varepsilon^2} Su_\varepsilon \right) + \alpha \beta \bar{E}_\varepsilon^{(k)}(f), \quad (46) \end{aligned}$$

and

$$\partial_t \bar{w}_\varepsilon^{(k)} + g \left(\bar{u}_\varepsilon^{(k)}, \bar{w}_\varepsilon^{(k)} \right) = \bar{E}_\varepsilon^{(k)}(g). \quad (47)$$

5.2 Definition of the two layers model

Consider some initial data $\hat{u}_0^{(k)}(x)$ and $\hat{w}_0^{(k)}(x)$ defined on ω . The two layers model is given by the following coupled systems of monodomain equations, for $k = 1, 2$:

$$\alpha \left(\partial_t \hat{u}_\varepsilon^{(k)} + \beta f \left(\hat{u}_\varepsilon^{(k)}, \hat{w}_\varepsilon^{(k)} \right) \right) = \operatorname{div}_x \left(\sigma^{(k)} \nabla_x \hat{u}_\varepsilon^{(k)} \right) + (-1)^k \frac{3}{2} \sigma_3^h \frac{\hat{u}_\varepsilon^{(1)} - \hat{u}_\varepsilon^{(2)}}{\varepsilon^2}, \quad (48)$$

$$\partial_t \hat{w}_\varepsilon^{(k)} + g \left(\hat{u}_\varepsilon^{(k)}, \hat{w}_\varepsilon^{(k)} \right) = 0, \quad (49)$$

with boundary conditions $\sigma^{(k)} \nabla_x \hat{u}^{(k)} \cdot n = 0$ on $\partial\omega$ for $t > 0$ and initial condition $\hat{u}^{(k)}(0, x) = \hat{u}_0^{(k)}(x)$ and $\hat{w}^{(k)}(0, x) = \hat{w}_0^{(k)}(x)$. It is a perturbation of the original problem (46)-(47). We are going to show that this perturbation is actually small.

5.3 Error estimate for the two layer model

We estimate the error between the solution $(\hat{u}_\varepsilon^{(k)}, \hat{w}_\varepsilon^{(k)})$ of the equations (48) and (49), and the averages, per layer, $(\bar{u}_\varepsilon^{(k)}, \bar{w}_\varepsilon^{(k)})$ of the solutions of the equations (12) and (13).

Theorem 3 (Error estimates for the two-layers model) *Assume that, for $k = 1, 2$, we have $\hat{u}_0^{(k)}(x) = u^0(x)$, and $\hat{w}_0^{(k)}(x) = w^0(x)$, and that $\left| \left(\hat{u}_\varepsilon^{(k)}(t, x), \hat{w}_\varepsilon^{(k)}(t, x) \right) \right| \leq M$ with the bound M from Theorem 1. Under the assumptions of Theorems 1 and 2, we have the following estimates: for all $0 < \varepsilon \leq 1$, for all $t > 0$, for $k = 1, 2$,*

$$\|\bar{u}_\varepsilon^{(k)}(t) - \hat{u}_\varepsilon^{(k)}(t)\|_{L^2(\omega)} \leq \varepsilon^3 k_4(t) \exp\left(\frac{c_2}{2}t\right), \quad (50)$$

$$\|\bar{w}_\varepsilon^{(k)}(t) - \hat{w}_\varepsilon^{(k)}(t)\|_{[L^2(\omega)]^m} \leq \varepsilon^3 k_4(t) \exp\left(\frac{c_2}{2}t\right), \quad (51)$$

$$\|\nabla_x(\bar{u}_\varepsilon^{(k)} - \hat{u}_\varepsilon^{(k)})\|_{L^2(0,T;L^2(\omega))} \leq \varepsilon^3 k_5(t) \exp\left(\frac{c_2}{2}t\right), \quad (52)$$

with $k_4(t) = \frac{1}{\sqrt{\alpha}} \left(\frac{d_4}{c_2} + \int_0^t d_5(s) ds \right)^{1/2}$, $k_5(t) = \frac{1}{\sqrt{2\alpha}} \left(\frac{d_4}{c_2} (1 + c_2 t) + 2 \int_0^t d_5(s) ds \right)^{1/2}$, and the constants $c_2 = 1 + 2\Lambda_0$, $d_4 = 4\alpha\Lambda_1^2 M^4 |\omega|$, and

$$d_5(t) = \frac{2\bar{\sigma}^2}{3\sigma_3^h \varepsilon^8} \sum_{k=1,2} \|\partial_{zz} e_\varepsilon^{(k)}\|_{L^2(\Omega^{(k)})}^2 + \frac{6\sigma_3^h}{\varepsilon^2} \sum_{k=1,2} \|\partial_z e_\varepsilon^{(k)}\|_{L^2(\Omega^{(k)})}^2 + 8\Lambda_0^2 \alpha k_0(t)^2 \exp(c_0 t).$$

The function $d_5(t)$ is such that $k_4(t)$ and $k_5(t)$ are bounded uniformly with respect to ε (see inequality (53)).

Proof:

We follow closely the method presented in the previous proofs. We subtract Equations (48) and (49) to Equations (46) and (47) and obtain, for $k = 1, 2$,

$$\alpha \left(\partial_t \hat{e}_\varepsilon^{(k)} + \beta \left(f(\bar{u}_\varepsilon^{(k)}, \bar{w}_\varepsilon^{(k)}) - f(\hat{u}_\varepsilon^{(k)}, \hat{w}_\varepsilon^{(k)}) \right) \right) = \operatorname{div}_x \left(\sigma^{(k)} \nabla_x \hat{e}_\varepsilon^{(k)} \right) + (-1)^k \frac{3}{2} \sigma_3^h \frac{\hat{e}_\varepsilon^{(1)} - \hat{e}_\varepsilon^{(2)}}{\varepsilon^2} + (-1)^k \frac{Ru_\varepsilon}{\varepsilon^2} + \alpha \beta \bar{E}_\varepsilon^{(k)}(f),$$

and

$$\partial_t \hat{f}_\varepsilon^{(k)} + g(\bar{u}_\varepsilon^{(k)}, \bar{w}_\varepsilon^{(k)}) - g(\hat{u}_\varepsilon^{(k)}, \hat{w}_\varepsilon^{(k)}) = \bar{E}_\varepsilon^{(k)}(g),$$

where $Ru_\varepsilon = Su_\varepsilon - \frac{3}{2}\sigma_3^h (\bar{e}_\varepsilon^{(1)} - \bar{e}_\varepsilon^{(2)})$ and with the notations $\hat{e}_\varepsilon^{(k)} = \bar{u}_\varepsilon^{(k)} - \hat{u}_\varepsilon^{(k)}$ and $\hat{f}_\varepsilon^{(k)} = \bar{w}_\varepsilon^{(k)} - \hat{w}_\varepsilon^{(k)}$. We multiply the equations by $\hat{e}_\varepsilon^{(k)}$ and $\alpha \hat{f}_\varepsilon^{(k)}$, integrate on ω , sum for $k = 1, 2$, and finally obtain the energy estimate,

$$\begin{aligned} \frac{1}{2} \frac{d}{dt} y(t) + \underline{\sigma} \sum_{k=1,2} \int_\omega |\nabla_x \hat{e}_\varepsilon^{(k)}|^2 dx + \frac{3}{2} \int_\omega \sigma_3^h \frac{|\hat{e}_\varepsilon^{(1)} - \hat{e}_\varepsilon^{(2)}|^2}{\varepsilon^2} dx \\ \leq \alpha \sum_{k=1,2} \int_\omega \hat{E}_\varepsilon^{(k)}(\beta f, g) \cdot (\hat{e}_\varepsilon^{(k)}, \hat{f}_\varepsilon^{(k)}) dx + \int_\omega \frac{Ru_\varepsilon}{\varepsilon^2} (\hat{e}_\varepsilon^{(2)} - \hat{e}_\varepsilon^{(1)}) dx \\ + \alpha \sum_{k=1,2} \int_\omega \bar{E}_\varepsilon^{(k)}(\beta f, g) \cdot (\hat{e}_\varepsilon^{(k)}, \hat{f}_\varepsilon^{(k)}) dx \end{aligned}$$

where $y(t) = \alpha \sum_{k=1,2} (\|\hat{e}_\varepsilon^{(k)}\|_{L^2(\omega)}^2 + \|\hat{f}_\varepsilon^{(k)}\|_{L^2(\omega)}^2) = \alpha \sum_{k=1,2} \|(\hat{e}_\varepsilon^{(k)}, \hat{f}_\varepsilon^{(k)})\|_{L^2(\omega)}^2$ and the nonlinear terms read $\hat{E}_\varepsilon^{(k)}(\beta f, g) = \mathbf{f}(\hat{u}_\varepsilon^{(k)}, \hat{w}_\varepsilon^{(k)}) - \mathbf{f}(\bar{u}_\varepsilon^{(k)}, \bar{w}_\varepsilon^{(k)})$, using the function $\mathbf{f}: (u, w) \in \mathbb{R} \times \mathbb{R}^m \mapsto (\beta f(u, w), g(u, w)) \in \mathbb{R} \times \mathbb{R}^m$. With the inequality of Young, we first remark that

$$\int_\omega \frac{Ru_\varepsilon}{\varepsilon^2} (\hat{e}_\varepsilon^{(2)} - \hat{e}_\varepsilon^{(1)}) dx \leq \frac{1}{2\gamma\varepsilon^2} \int_\omega |Ru_\varepsilon|^2 dx + \frac{\gamma}{2\varepsilon^2} \int_\omega (\hat{e}_\varepsilon^{(2)} - \hat{e}_\varepsilon^{(1)})^2 dx.$$

We take $\gamma = \frac{3}{2}\sigma_3^h$, in order to simplify this term with the left-hand side of the equation, and obtain the estimate:

$$\begin{aligned} \frac{1}{2} \frac{d}{dt} y(t) + \underline{\sigma} \sum_{k=1,2} \int_\omega |\nabla_x \hat{e}_\varepsilon^{(k)}|^2 dx + \frac{3}{4} \int_\omega \sigma_3^h \frac{|\hat{e}_\varepsilon^{(1)} - \hat{e}_\varepsilon^{(2)}|^2}{\varepsilon^2} dx \\ \leq \frac{1}{3\sigma_3^h \varepsilon^2} \int_\omega |Ru_\varepsilon|^2 dx + \alpha \sum_{k=1,2} \int_\omega (\hat{E}_\varepsilon^{(k)}(\beta f, g) + \bar{E}_\varepsilon^{(k)}(\beta f, g)) \cdot (\hat{e}_\varepsilon^{(k)}, \hat{f}_\varepsilon^{(k)}) dx. \end{aligned}$$

We are going to bound independently each element of the right hand side of this inequality. Firstly, we have:

$$\begin{aligned} \frac{1}{3\sigma_3^h \varepsilon^2} \int_\omega |Ru_\varepsilon|^2 dx &\leq \frac{1}{3\sigma_3^h \varepsilon^2} \int_\omega \left| Su_\varepsilon - \frac{3}{2}\sigma_3^h (\bar{e}_\varepsilon^{(1)} - \bar{e}_\varepsilon^{(2)}) \right|^2 dx \\ &\leq \frac{2}{3\sigma_3^h \varepsilon^2} \int_\omega |Su_\varepsilon|^2 dx + \frac{3}{2} \int_\omega \sigma_3^h \frac{|\bar{e}_\varepsilon^{(1)} - \bar{e}_\varepsilon^{(2)}|^2}{\varepsilon^2} dx. \end{aligned}$$

Now recall Equation (45) that defines Su_ε and note that, for all $t > 0$, for a.e. $x \in \omega$, we have $\partial_z e^{(1)}(t, x, 0) = -\int_0^1 \partial_{zz} e^{(1)}(t, x, z) dz$ so that

$$\int_\omega |Su_\varepsilon|^2 dx \leq \int_\omega \sigma_3^{(1)2} \left| \int_0^1 \partial_{zz} e_\varepsilon^{(1)} dz \right|^2 dx \leq \bar{\sigma}^2 \|\partial_{zz} e_\varepsilon^{(1)}\|_{L^2(\Omega^{(1)})}^2.$$

Here, the choice of $e_\varepsilon^{(1)}$ is arbitrary and could be replaced by $e_\varepsilon^{(2)}$ because of the continuity of the flux through $\Sigma = \omega \times \{0\}$. As a consequence, we also have $\int_\omega |Su_\varepsilon|^2 dx \leq \frac{1}{2} \bar{\sigma}^2 \sum_{k=1,2} \|\partial_{zz} e_\varepsilon^{(k)}\|_{L^2(\Omega^{(k)})}^2$. Afterwards, because of the continuity of $e_\varepsilon^{(k)}$ along the interface $\{z=0\}$, we have (using Lemma 2):

$$\begin{aligned} \int_\omega \left| \bar{e}_\varepsilon^{(1)} - \bar{e}_\varepsilon^{(2)} \right|^2 dx & \leq 2 \int_\omega \left(\left| \bar{e}_\varepsilon^{(1)}(t,x) - e_\varepsilon^{(1)}(t,x,0) \right|^2 + \left| \bar{e}_\varepsilon^{(2)}(t,x) - e_\varepsilon^{(2)}(t,x,0) \right|^2 \right) dx \\ & \leq 2 \int_\omega \left(\left| \int_0^1 \partial_z e^{(1)} dz \right|^2 + \left| \int_0^1 \partial_z e^{(2)} dz \right|^2 \right) dx \leq 2 \sum_{k=1,2} \|\partial_z e^{(k)}\|_{L^2(\Omega^{(k)})}^2. \end{aligned}$$

We finally have:

$$\frac{1}{3\sigma_3^h \varepsilon^2} \int_\omega |Ru_\varepsilon|^2 dx \leq \frac{2\bar{\sigma}^2}{3\sigma_3^h \varepsilon^2} \sum_{k=1,2} \|\partial_{zz} e_\varepsilon^{(k)}\|_{L^2(\Omega^{(k)})}^2 + \frac{3\sigma_3^h}{\varepsilon^2} \sum_{k=1,2} \|\partial_z e^{(k)}\|_{L^2(\Omega^{(k)})}^2.$$

Secondly, we have $\left| \hat{E}_\varepsilon^{(k)}(\beta f, g) \right| = \left| \mathbf{f}(\bar{u}_\varepsilon^{(k)}, \bar{w}_\varepsilon^{(k)}) - \mathbf{f}(\hat{u}_\varepsilon^{(k)}, \hat{w}_\varepsilon^{(k)}) \right| \leq \Lambda_0 \left| \left(\hat{e}_\varepsilon^{(k)}, \hat{f}_\varepsilon^{(k)} \right) \right|$, and then:

$$\left| \alpha \sum_{k=1,2} \int_\omega \hat{E}_\varepsilon^{(k)}(\beta f, g) \cdot \left(\hat{e}_\varepsilon^{(k)}, \hat{f}_\varepsilon^{(k)} \right) dx \right| \leq \alpha \Lambda_0 \sum_{k=1,2} \int_\omega \left| \left(\hat{e}_\varepsilon^{(k)}, \hat{f}_\varepsilon^{(k)} \right) \right|^2 dx = \Lambda_0 y(t).$$

Lastly, we recall that $(\bar{u}_\varepsilon^{(k)}, \bar{w}_\varepsilon^{(k)}) = (u_0, w_0) + \varepsilon^2 (u_1^{(k)}, w_1^{(k)})$, and then $(\bar{\bar{u}}_\varepsilon^{(k)}, \bar{\bar{w}}_\varepsilon^{(k)}) = (u_0, w_0) + \varepsilon^2 (\bar{u}_1^{(k)}, \bar{w}_1^{(k)})$ are the integrals of $(\bar{u}_\varepsilon^{(k)}, \bar{w}_\varepsilon^{(k)})$ in z , and we compute:

$$\begin{aligned} \bar{E}_\varepsilon^{(k)}(\beta f, g) & = \left(\mathbf{f}(\bar{u}_\varepsilon^{(k)}, \bar{w}_\varepsilon^{(k)}) - \mathbf{f}(\bar{\bar{u}}_\varepsilon^{(k)}, \bar{\bar{w}}_\varepsilon^{(k)}) \right) \\ & \quad + \left(\mathbf{f}(\bar{\bar{u}}_\varepsilon^{(k)}, \bar{\bar{w}}_\varepsilon^{(k)}) - \mathbf{f}(u_0, w_0) - \varepsilon^2 \nabla \mathbf{f}(u_0, w_0) \cdot \left(\bar{u}_1^{(k)}, \bar{w}_1^{(k)} \right) \right) \\ & \quad + \left(\mathbf{f}(u_0, w_0) + \varepsilon^2 \nabla \mathbf{f}(u_0, w_0) \cdot \left(\bar{u}_1^{(k)}, \bar{w}_1^{(k)} \right) - \overline{\mathbf{f}(u_\varepsilon^{(k)}, w_\varepsilon^{(k)})} \right). \end{aligned}$$

For these three terms, we have (Lipschitz continuity of \mathbf{f}):

$$\left| \mathbf{f}(\bar{u}_\varepsilon^{(k)}, \bar{w}_\varepsilon^{(k)}) - \mathbf{f}(\bar{\bar{u}}_\varepsilon^{(k)}, \bar{\bar{w}}_\varepsilon^{(k)}) \right| \leq \Lambda_0 \left| \left(\bar{e}_\varepsilon^{(k)}, \bar{f}_\varepsilon^{(k)} \right) \right| \leq \Lambda_0 \int_0^1 \left| \left(e_\varepsilon^{(k)}, f_\varepsilon^{(k)} \right) \right| dz$$

if $k=1$ and the same for $z \in (-1, 0)$ if $k=2$, and (Lemma 1):

$$\begin{aligned} \left| \mathbf{f}(\bar{\bar{u}}_\varepsilon^{(k)}, \bar{\bar{w}}_\varepsilon^{(k)}) - \mathbf{f}(u_0, w_0) - \varepsilon^2 \nabla \mathbf{f}(u_0, w_0) \cdot \left(\bar{u}_1^{(k)}, \bar{w}_1^{(k)} \right) \right| \\ = \left| I_{\mathbf{f}} \left((u_0, w_0), (\bar{\bar{u}}_\varepsilon^{(k)}, \bar{\bar{w}}_\varepsilon^{(k)}) \right) \right| \leq \frac{1}{2} \Lambda_1 \varepsilon^4 \left| \left(\bar{u}_1^{(k)}, \bar{w}_1^{(k)} \right) \right|^2 \leq \frac{1}{2} \Lambda_1 \varepsilon^4 M^2, \end{aligned}$$

and, at last (for the case $k=1$ – application of the estimate (39)):

$$\begin{aligned} \left| \mathbf{f}(u_0, w_0) + \varepsilon^2 \nabla \mathbf{f}(u_0, w_0) \cdot \left(\bar{u}_1^{(k)}, \bar{w}_1^{(k)} \right) - \overline{\mathbf{f}(u_\varepsilon^{(k)}, w_\varepsilon^{(k)})} \right| \\ \leq \int_0^1 \left| \mathbf{f}(u_0, w_0) + \varepsilon^2 \nabla \mathbf{f}(u_0, w_0) \cdot \left(u_1^{(1)}, w_1^{(1)} \right) - \mathbf{f}(u_\varepsilon^{(1)}, w_\varepsilon^{(1)}) \right| dz \\ \leq \int_0^1 \Lambda_0 \left| \left(e_\varepsilon^{(k)}, f_\varepsilon^{(k)} \right) \right| dz + \frac{1}{2} \Lambda_1 \varepsilon^4 M^2, \end{aligned}$$

and the same estimate holds for the case $k = 2$. In consequence, we have (for $k = 1$ – the integral is on $z \in (-1, 0)$ for $k = 2$):

$$\left| \bar{E}_\varepsilon^{(k)}(\beta f, g) \right| \leq \Lambda_1 \varepsilon^4 M^2 + 2\Lambda_0 \int_0^1 \left| \left(e_\varepsilon^{(k)}, f_\varepsilon^{(k)} \right) \right| dz.$$

Hence, we find that:

$$\begin{aligned} & \left| \alpha \sum_{k=1,2} \int_\omega \bar{E}_\varepsilon^{(k)}(\beta f, g) \cdot \left(\hat{e}_\varepsilon^{(k)}, \hat{f}_\varepsilon^{(k)} \right) dx \right| \\ & \leq \frac{\alpha}{2} \sum_{k=1,2} \left(\int_\omega \left| \bar{E}_\varepsilon^{(k)}(\beta f, g) \right|^2 dx + \int_\omega \left| \hat{e}_\varepsilon^{(k)}, \hat{f}_\varepsilon^{(k)} \right|^2 dx \right) \\ & \leq \alpha \sum_{k=1,2} \left(\Lambda_1^2 \varepsilon^8 M^4 |\omega| + 4\Lambda_0^2 \int_{\Omega^{(k)}} \left| \left(e_\varepsilon^{(k)}, f_\varepsilon^{(k)} \right) \right|^2 dz dx \right) + \frac{1}{2} y(t) \\ & \leq 2\alpha \Lambda_1^2 \varepsilon^8 M^4 |\omega| + 4\Lambda_0^2 \alpha k_0(t)^2 \varepsilon^6 \exp(c_0 t) + \frac{1}{2} y(t) \end{aligned}$$

applying the results of Theorem 1. The final energy estimate reads (for $0 < \varepsilon \leq 1$):

$$\begin{aligned} \frac{d}{dt} y(t) + 2\bar{\sigma} \sum_{k=1,2} \int_\omega \left| \nabla_x \hat{e}_\varepsilon^{(k)} \right|^2 dx + \frac{3}{2} \sigma_3^h \int_\omega \sigma_3^h \frac{\left| \hat{e}_\varepsilon^{(1)} - \hat{e}_\varepsilon^{(2)} \right|^2}{\varepsilon^2} dx \\ \leq c_2 y(t) + \varepsilon^6 (d_4 + d_5(t)) \end{aligned}$$

where the constant c_2 , d_4 and the function $d_5(t)$ are given in the statement of Theorem 3. Using again Lemma 3, this proves the result, because, for all $t > 0$ and $0 < \varepsilon \leq 1$, due to the inequalities (35) and (43) from Theorems 1 and 2,

$$\begin{aligned} \int_0^t d_5(s) ds &= 8\Lambda_0^2 \alpha \int_0^t k_0(s)^2 \exp(c_0 s) ds \\ &+ \frac{2\bar{\sigma}^2}{3\sigma_3^h \varepsilon^8} \sum_{k=1,2} \|\partial_{zz} e_\varepsilon^{(k)}\|_{L^2(0,t;L^2(\Omega^{(k)}))}^2 + \frac{6\sigma_3^h}{\varepsilon^8} \sum_{k=1,2} \|\partial_z e_\varepsilon^{(k)}\|_{L^2(0,t;L^2(\Omega^{(k)}))}^2 < +\infty, \end{aligned} \quad (53)$$

and then $k_4(t)$ and $k_5(t)$ are bounded with respect to ε for all $t > 0$.

□

Remark 5 *This theorem guarantees that the average by layer in the thickness of the three-dimensional potential converges toward the solution of the two-layers model. Furthermore, the accuracy of the two-layers model is limited by the precision of the approximation of the transverse diffusion which depends in our formulation on the precision of the asymptotic expansion of $u_\varepsilon^{(k)}$.*

Let us give a version of the problem (48) in physical variables :

$$A(C\partial_t u^{(k)} + f(u^{(k)}, w^{(k)})) = \operatorname{div}_x(\sigma^{(k)} \nabla_x u^{(k)}) + (-1)^k \sigma_3^h (u^{(1)} - u^{(2)}), \quad (54)$$

$$\partial_t w^{(k)} + g(u^{(k)}, w^{(k)}) = 0 \quad (55)$$

where $\sigma_3^h = \frac{3}{h^2} \frac{\sigma_3^{(1)} \sigma_3^{(2)}}{\sigma_3^{(1)} + \sigma_3^{(2)}}$ is called the coupling coefficient and $A, C, \sigma^{(k)}, \sigma_3^{(k)}$ are the same parameters than in problem (1,2).

$2h$	x_0	T	A	C	$\sigma_1^{(k)}$	$\sigma_2^{(k)}$	$\sigma_3^{(k)}$	$\theta^{(1)}$	$\theta^{(2)}$
cm	cm	ms	cm ⁻¹	μFcm^{-2}		mScm^{-1}			
[0.01, 0.4]	1	400	500	1	1.5	0.2	0.2	0	$\pi/2$

Table 2: Parameters of the equations

Remark 6 *The model also has a purely electric interpretation, as in [Jacquemet, 2004]: the two layers are coupled pointwise by a conductance. The coupling coefficient from our model, σ_3^h , is expressed in mScm^{-2} , which is consistent. Consequently, the term $\sigma_3^h(u^{(1)} - u^{(2)})$ is a density of current expressed in μAcm^{-2} .*

6 Numerical illustrations

6.1 The test cases

We want to simulate the propagation of the activation front on a three-dimensional slab of tissue $\Omega = \omega \times (-h, h)$ for various values of the thickness parameter $h > 0$, and with a discontinuity through the surface $\{z = 0\}$. We take $\omega = (0, x_0) \times (0, x_0)$ and define the conductivity matrices $\sigma^{(k)}$ in the layers $\Omega^{(k)}$ following equations (6) with fiber direction as in equations (5). We have the choice between three models:

3D: The complete three-dimensional equations (1) and (2) on Ω , or the equivalent systems of equations (7) and (8) on the layers $\Omega^{(k)}$, which solutions are denoted by $u_h^{(k)}$ and $w_h^{(k)}$;

2Dx1: The order 0 term of the asymptotic expansion, u_0 and w_0 , that solve the usual surface monodomain equation (22) and (23) on ω and does not depend on h ;

2Dx2: The solution of the two-layers model, $\hat{u}_h^{(k)}$ and $\hat{w}_h^{(k)}$, that solve the equations (54) and (55) on ω with the coupling parameter $\sigma_3^h = \frac{3}{h^2} \frac{\sigma_3^{(1)} \sigma_3^{(2)}}{\sigma_3^{(1)} + \sigma_3^{(2)}}$.

The functions f and g are defined by the Beeler-Reuter ionic model [Beeler and Reuter, 1977], for it is computationally simple but retains the essential features of the cardiac action potential. The angles $\theta^{(k)}$ of the fibers in layers $k = 1$ and 2 , and the remaining parameters of the equations are given in table 2. We will explore values of the thickness parameter h ranging from the typical diameter of a cardiomyocyte (tens of μm) up to large atrial thickness (less than a cm) as found in humans.

An action potential is initiated by applying a transmembrane voltage of 20mV during a period of 2ms in the domain $S = (0.49x_0, 0.51x_0) \times (0.49x_0, 0.51x_0)$ for the surface models and in the cylinder $S \times (-h, h)$ for the 3D model.

6.2 Meshes, discretization, and resolution

We consider a Cartesian grid of Ω with space steps $\Delta x \times \Delta x \times \Delta z$ in the directions x , y , and z ; and the subgrid with space steps $\Delta x \times \Delta x$ of ω . These Cartesian grids are split into a simplicial mesh of Ω (that is with tetrahedra) and a simplicial submesh for ω (that is with triangles), by splitting each square into 4 triangles and each hexahedron into 24 tetrahedra (see Figure 1). In order to guarantee the convergence of the discrete solution, we take $\Delta x = x_0/200 = 5.e - 3\text{cm}$ and Δz is chosen as in table 3. This choice guarantees that there are at least 10 elements through the whole thickness of Ω (that is $2h$) and $\Delta z \leq 4\Delta x$.

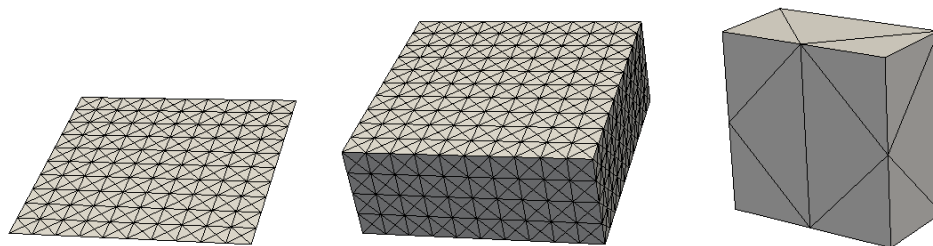


Figure 1: Left: mesh of ω . Middle : mesh of Ω . Right : each hexahedron is split into 24 tetrahedra

The equations (1), (2) for the three-dimensional model, (54), (55) for the two-layers model, and (22), (23) for the usual surface model are discretized by using the standard P1-Lagrange finite element method in space with diagonal mass lumping (due to the numerical quadrature rule) and the Rush-Larsen time-stepping scheme [Rush and Larsen, 1978] with the fixed time-step $\Delta t = 0.05\text{ms}$. During the Rush-Larsen iteration, the diffusion terms are solved implicitly; so are the coupling terms in the coupled equations of the two-layers model. All the linear systems are solved with a conjugate gradient method, a Jacobi preconditionner, and a fixed tolerance equal to $1.e - 10$.

$2h$	0.4	0.3	0.2	0.1	0.09	0.08
Δz	0.02	0.015	0.01	0.01	0.009	0.008
#dof 2Dx1	80 401	80 401	80 401	80 401	80 401	80 401
#dof 2Dx2	160 802	160 802	160 802	160 802	160 802	160 802
#dof 3D	3 296 421	3 296 421	3 296 421	1 688 411	1 688 411	1 688 411

0.07	0.06	0.05	0.04	0.03
0.007	0.006	0.005	0.004	0.003
80 401	80 401	80 401	80 401	80 401
160 802	160 802	160 802	160 802	160 802
1 688 411	1 688 411	1 688 411	1 688 411	1 688 411

Table 3: Meshes and numbers of degrees of freedom.

The objective of our study is not to investigate the numerical method but to study the impact of the modeling choices that we propose.

6.3 Numerical results

6.3.1 Qualitative behavior

For two values of the thickness parameter, corresponding to the asymptotic ($2h = 0.03\text{cm}$) and non-asymptotic ($2h = 0.1\text{cm}$) regimes, we display, for each layer, the average $\bar{u}_h^{(k)}(x)$ of the three-dimensional solution $u_h^{(k)}(x, z)$, the two-dimensional solution $\hat{u}_h^{(k)}(x)$, and the surface solution $u_0(x)$ of our three models

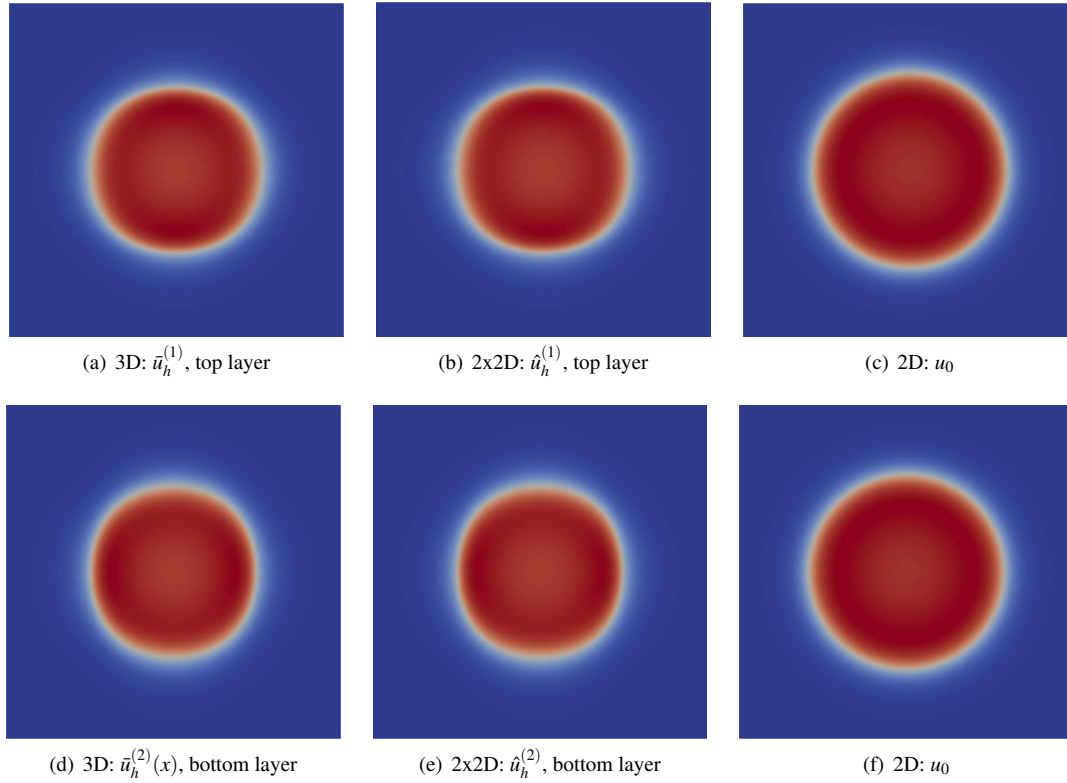


Figure 2: Solutions in the asymptotic regime, $2h = 0.03\text{cm}$.

(Figures 2 and 3). All solutions are displayed at time $t = 9\text{ms}$. In the asymptotic regime, all solutions are qualitatively very similar (Figure 2), as expected. In the non-asymptotic regime, the usual surface model clearly misses the important three-dimensional interplay of diffusion and reaction between the two distinct layers of tissue. This interplay induces the diamond-shaped wavefront seen on Figure 3, that remains in our two-layers surface model, but not in the usual surface model. Note that such a wavefront was observed experimentally in [Vetter et al., 2005]. Our two-layers model clearly accounts for such phenomena.

6.3.2 Errors

In order to quantify the distances from the surface model or our two-layers model, to the three-dimensional one, and accordingly with the results from theorems 1 and 3, we define the following errors E_0 and E_1 :

$$E_0(h) = \frac{\max_n \|\bar{u}_h^n - u_0^n\|_{L^2(\omega)}}{\max_n \|\bar{u}_h^n\|_{L^2(\omega)}}, \quad E_1(h) = \frac{\max_n \|\bar{u}_h^{(k),n} - \hat{u}_h^{(k),n}\|_{L^2(\omega)}}{\max_n \|\bar{u}_h^{(k),n}\|_{L^2(\omega)}} \quad (56)$$

where $\bar{u}_h^n = \frac{1}{2} (\bar{u}_h^{(1),n} + \bar{u}_h^{(2),n})$, u_0^n , $\bar{u}_h^{(k),n}$, and $\hat{u}_h^{(k),n}$ refer to the discrete solutions of the models at time $t^n = n\Delta t$

We expect that $E_0(h) = O(h^2)$ and $E_1(h) = O(h^3)$, although we presume that $E_1(h) = O(h^4)$ is the correct convergence rate (remark 5). The error graphs $(h, E_0(h))$ and $(h, E_1(h))$ are displayed on the

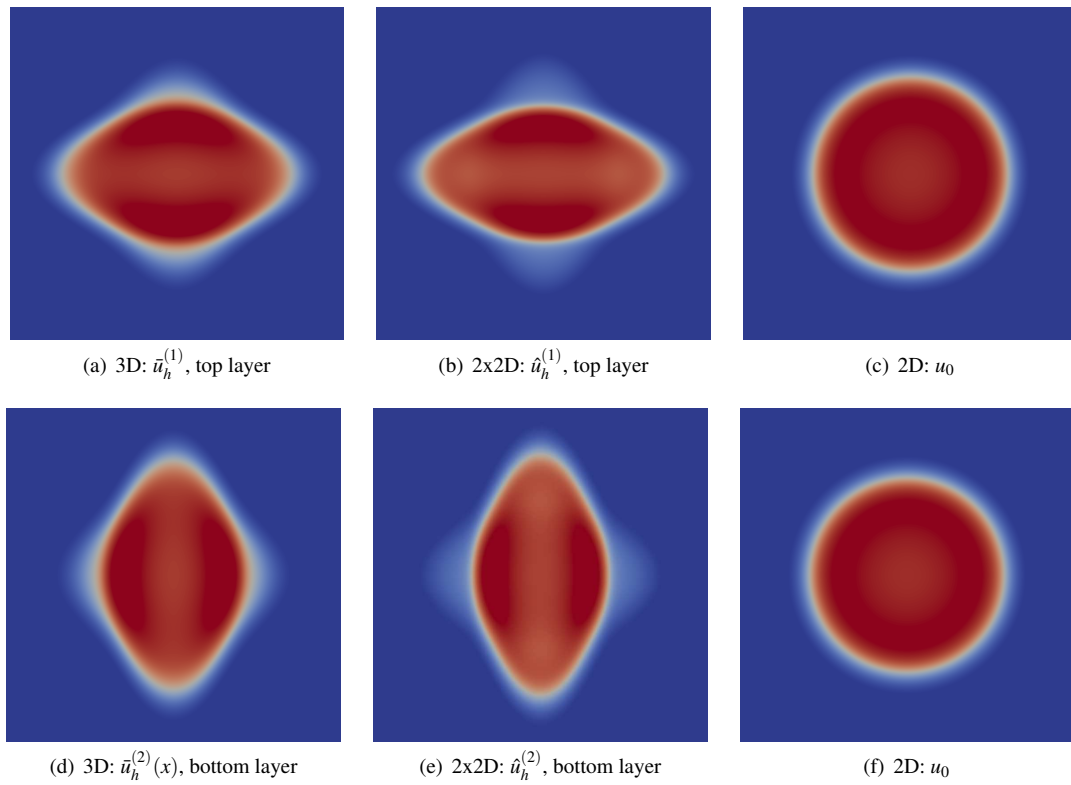


Figure 3: Solutions in the physiologic regime, $2h = 0.1\text{cm}$.

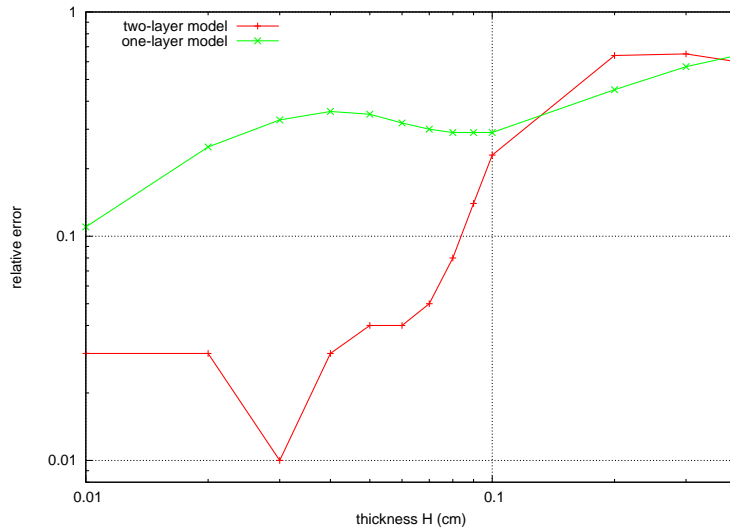


Figure 4: Errors $E_0(h)$ and $E_1(h)$ defined in equation (56).

Figure 4. As expected, we observe the convergence of both models, and a higher convergence rate for the two-layers model ($E_1(h)$) than for the surface model ($E_0(h)$), but only for $h < 0.1$ cm.

Finally, table (3) shows the very strong improvement of the computational cost for the two-layers (25 to 70 times faster), and the usual surface (70 to 170 times faster) models.

h	0.4	0.1
2Dx1	0.0069	0.0127
2Dx2	0.0171	0.0310

Table 4: Ratio of cpu time for the surface models with respect to the three-dimensional computation cpu time, for the two different three-dimensional discretisation.

7 Conclusion

7.1 Interest of two-layers model

A similar two-layers model was proposed in [Jacquemet, 2004, Gharaviri et al., 2012], but its rigorous mathematical derivation, the error estimates proved in Theorem 3, and the numerical study from section 6 are new. In addition, the dimensional analysis from section 3.1 gives a good understanding of how the trade-off between reaction and diffusion could trigger complex three-dimensional propagation patterns.

The main advantage of the bilayer model over the usual surface model resides in the distinction of individual reaction terms and diffusion terms in the layers. This is important to trigger transmural gradients and dissociation of the electrical activity, together with complex anisotropic propagation patterns

as observed in [Vetter et al., 2005]. The usual surface model, even enhanced by addition of the second order term $\varepsilon^2 u_1^{(k)}$ would not easily account for these phenomena. Yet, we point out that these phenomena (dissociation, transmural gradients, complex propagation) are expected to play a major role in the initiation of arrhythmias. Hence, the two-layers model is a very efficient tool to investigate in depth the arrhythmogenic mechanisms in the atria.

At last, the computational costs of the two-layers model is divided by 50 (on average) with respect to the cost of three-dimensional model.

7.2 Limitations and perspectives

Although being a strong qualitative enhancement of the usual surface model, the two-layers model could still be improved, for instance by incorporating higher order terms in the Taylor expansions. The derivation of a more general bidomain version of the two layers model on more general geometries is also possible, following the work from [Chapelle et al., 2013]. Furthermore, other relative balance between diffusion and reaction as mentioned in Remark 5 can be studied based on a different adimensionalization.

Our numerical study illustrates the results from section 4.1 and 5 and we give errors in the L^2 norm. For medical issues, activation maps and numerical errors on the activation times have to be derived.

Mechanisms well rendered by the two-layers model (dissociation, transmural gradient...) occur only in small localized parts of the atria, with abrupt variation of the fiber orientation and thin tissues. These configurations are found in the pulmonary veins and in some areas of the atrial chambers such as the left atrium posterior and anterior walls or the pectinate muscles, and the Crista terminalis in the right atrium. Hence, coupling the two-layers model to the usual surface model might improve the computational efficiency of the overall method.

Beyond its mathematical derivation, this two-layers model is interesting to construct anatomically and structurally accurate models of the human atria: clinical images give the two-dimensional surfaces, that are completed by histological descriptions such as [Ho et al., 2002] or [Ho et al., 1999]. We believe that it will become an appreciated tool to study the structure-to-function relations in the atria, from a medical point of view. A first model therefore was presented in [Vigmond et al., 2013, Labarthe et al., 2013].

acknowledgements:

We used the experimental testbed PLAFRIM (see <https://plafrim.bordeaux.inria.fr>) to complete the computations presented in the article.

This work was partially supported by an ANR grant part of "Investissements d'Avenir" program with reference ANR-10-IAHU-04, and by the Region Aquitaine.

□

A Proof of Lemma 4

For all $t > 0$ and a.e. $x \in \omega$, according to the equation (13) on $w_\varepsilon^{(k)}$, we have, for $k = 1, 2$,

$$\partial_t w_\varepsilon^{(k)}(t, x, 0) + g\left(u_\varepsilon^{(k)}(t, x, 0), w_\varepsilon^{(k)}(t, x, 0)\right) = 0.$$

We test these equations against the function $\left(w_\varepsilon^{(1)} - w_\varepsilon^{(2)}\right)(t, x, 0)$ and subtract them one with another, in order to get

$$\frac{1}{2} \frac{d}{dt} \int_\omega \left|w_\varepsilon^{(1)} - w_\varepsilon^{(2)}\right|^2 dx \leq \Lambda_0 \int_\omega \left|w_\varepsilon^{(1)} - w_\varepsilon^{(2)}\right|^2 dx$$

because $u_\varepsilon^{(1)}(t, x, 0) = u_\varepsilon^{(2)}(t, x, 0)$ for $x \in \omega$, and where the constant Λ_0 is the one used in the proof of Theorem 1, that bounds also the Lipschitz constant of the function $w \mapsto g(u, w)$ for $|(u, w)| \leq 2M$. Since $w_\varepsilon^{(1)}(0, x, 0) = w_\varepsilon^{(2)}(0, x, 0)$ for a.e. $x \in \omega$, we see that $\int_\omega |w_\varepsilon^{(1)} - w_\varepsilon^{(2)}|^2 dx = 0$ for all $t > 0$, and hence $w_\varepsilon^{(1)} = w_\varepsilon^{(2)}$ on the interface $\Sigma = \omega \times \{0\}$.

After differentiation in z of equation (13), we find that, for $k = 1, 2$,

$$\partial_t \partial_z w_\varepsilon^{(k)}(t, x, 0) + \nabla g \left(u_\varepsilon^{(k)}(t, x, 0), w_\varepsilon^{(k)}(t, x, 0) \right) \cdot \left(\partial_z u_\varepsilon^{(k)}(t, x, 0), \partial_z w_\varepsilon^{(k)}(t, x, 0) \right) = 0.$$

We multiply these equations by $\sigma_3^{(k)}$, test them against $\left(\sigma_3^{(1)} w_\varepsilon^{(1)} - \sigma_3^{(2)} w_\varepsilon^{(2)} \right)(t, x, 0)$ and subtract them one with another, in order to get, for all $t > 0$,

$$\begin{aligned} & \frac{1}{2} \frac{d}{dt} \int_\omega \left| \sigma_3^{(2)} \partial_z w_\varepsilon^{(2)} - \sigma_3^{(1)} \partial_z w_\varepsilon^{(1)} \right|^2 dx \\ & \leq - \int_\omega \left(\nabla g(u_\varepsilon^{(2)}, w_\varepsilon^{(2)}) \left(\sigma_3^{(2)} \partial_z u_\varepsilon^{(2)}, \sigma_3^{(2)} \partial_z w_\varepsilon^{(2)} \right) \right. \\ & \quad \left. - \nabla g(u_\varepsilon^{(1)}, w_\varepsilon^{(1)}) \left(\sigma_3^{(1)} \partial_z u_\varepsilon^{(1)}, \sigma_3^{(1)} \partial_z w_\varepsilon^{(1)} \right) \right) \left(\sigma_3^{(2)} \partial_z w_\varepsilon^{(2)} - \sigma_3^{(1)} \partial_z w_\varepsilon^{(1)} \right) dx \\ & \leq \Lambda_0 \int_\omega \left| \sigma_3^{(2)} \partial_z w_\varepsilon^{(2)} - \sigma_3^{(1)} \partial_z w_\varepsilon^{(1)} \right|^2 dx \end{aligned}$$

because $u_\varepsilon^{(1)} = u_\varepsilon^{(2)}$, $w_\varepsilon^{(1)} = w_\varepsilon^{(2)}$, and $\sigma_3^{(1)} \partial_z u_\varepsilon^{(1)} = \sigma_3^{(2)} \partial_z u_\varepsilon^{(2)}$ on $\Sigma = \omega \times \{0\}$, and because Λ_0 bounds $|\nabla g(u, w)|$ for $|(u, w)| \leq 2M$. Like above, $\sigma_3^{(2)} \partial_z w_\varepsilon^{(2)} = \sigma_3^{(1)} \partial_z w_\varepsilon^{(1)}$ on $\Sigma = \omega \times \{0\}$ for all $t > 0$ because it is true for $t = 0$.

References

- G. W. Beeler and H. Reuter. Reconstruction of the action potential of ventricular myocardial fibres. *The Journal of Physiology*, 268(1):177–210, June 1977. URL <http://jp.physoc.org/content/268/1/177>.
- Mostafa Bendahmane and Kenneth H. Karlsen. Analysis of a class of degenerate reaction-diffusion systems and the bidomain model of cardiac tissue. *NETWORKS AND HETEROGENEOUS MEDIA*, 1(1):185–218, march 2006.
- Muriel Boulakia, Serge Cazeau, Miguel Fernández, Jean-Frédéric Gerbeau, and Nejib Zemzemi. Mathematical modeling of electrocardiograms: A numerical study. *Annals of Biomedical Engineering*, 38: 1071–1097, 2010. ISSN 0090-6964. URL <http://dx.doi.org/10.1007/s10439-009-9873-0>.
- John W. Cain. Criterion for stable reentry in a ring of cardiac tissue. *Journal of Mathematical Biology*, 55(3):433–448, 2007. ISSN 0303-6812. doi: 10.1007/s00285-007-0100-z. URL <http://dx.doi.org/10.1007/s00285-007-0100-z>.
- Dominique Chapelle, Annabelle Collin, and Jean-Frédéric Gerbeau. A surface-based electrophysiology model relying on asymptotic analysis and motivated by cardiac atria modeling. *Mathematical Models and Methods in Applied Sciences*, 2013. doi: 10.1142/S0218202513500450. URL <http://hal.inria.fr/hal-00723691>.

- John C. Clements, Jukka Nenonen, P. K. J. Li, and B. Milan Horacek. Activation dynamics in anisotropic cardiac tissue via decoupling. *Annals of Biomedical Engineering*, 32:984–990, 2004. ISSN 0090-6964. URL <http://dx.doi.org/10.1023/B:ABME.0000032461.80932.eb>. 10.1023/B:ABME.0000032461.80932.eb.
- L. Clerc. Directional differences of impulse spread in trabecular muscle from mammalian heart. *The Journal of Physiology*, 255:335–346, February 1 1976.
- P. Colli Franzone, L. Guerri, and S. Rovida. Wavefront propagation in an activation model of the anisotropic cardiac tissue: asymptotic analysis and numerical simulations. *Journal of Mathematical Biology*, 28:121–176, 1990. ISSN 0303-6812. URL <http://dx.doi.org/10.1007/BF00163143>. 10.1007/BF00163143.
- L. Dang, N. Virag, Z. Ihara, V. Jacquemet, J.-M. Vesin, J. Schlaepfer, P. Ruchat, and L. Kappenberger. Evaluation of ablation patterns using a biophysical model of atrial fibrillation. *Annals of Biomedical Engineering*, 33:465–474, 2005. ISSN 0090-6964. URL <http://dx.doi.org/10.1007/s10439-005-2502-7>. 10.1007/s10439-005-2502-7.
- Weber dos Santos and F. Dickstein. On the influence of a volume conductor on the orientation of currents in a thin cardiac issue. In Isabelle Magnin, Johan Montagnat, Patrick Clarysse, Jukka Nenonen, and Toivo Katila, editors, *Functional Imaging and Modeling of the Heart*, volume 2674 of *Lecture Notes in Computer Science*, pages 1009–1009. Springer Berlin / Heidelberg, 2003.
- Jens Eckstein, Bart Maesen, Dominik Linz, Stef Zeemering, Arne van Hunnik, Sander Verheule, Maurits Allesie, and Ulrich Schotten. Time course and mechanisms of endo-epicardial electrical dissociation during atrial fibrillation in the goat. *Cardiovascular Research*, 89(4):816–824, 2011. doi: 10.1093/cvr/cvq336. URL <http://cardiovascres.oxfordjournals.org/content/89/4/816.abstract>.
- Ali Gharaviri, Sander Verheule, Jens Eckstein, Mark Potse, Nico H.L. Kuijpers, and Ulrich Schotten. A computer model of endo-epicardial electrical dissociation and transmural conduction during atrial fibrillation. *Europace*, 14(suppl 5):v10–v16, 2012. doi: 10.1093/europace/eus270. URL http://europace.oxfordjournals.org/content/14/suppl_5/v10.abstract.
- Michel Haissaguerre, Kang-Teng Lim, Vincent Jacquemet, Martin Rotter, Lam Dang, Méléze Hocini, Seiichiro Matsuo, Sébastien Knecht, Pierre Jaïs, and Nathalie Virag. Atrial fibrillatory cycle length: computer simulation and potential clinical importance. *Europace*, 9(suppl 6):vi64–vi70, 2007. doi: 10.1093/europace/eum208. URL http://europace.oxfordjournals.org/content/9/suppl_6/vi64.abstract.
- S Y Ho, J A Cabrera, V H Tran, J Farré, R H Anderson, and D Sánchez-Quintana. Architecture of the pulmonary veins: relevance to radiofrequency ablation. *Heart*, 86(3):265–270, 2001. doi: 10.1136/heart.86.3.265. URL <http://heart.bmj.com/content/86/3/265.abstract>.
- Siew Yen Ho, Robert H. Anderson, and Damián Sánchez-Quintana. Atrial structure and fibres: morphologic bases of atrial conduction. *Cardiovascular Research*, 54(2):325–336, 2002. doi: 10.1016/S0008-6363(02)00226-2. URL <http://cardiovascres.oxfordjournals.org/content/54/2/325.abstract>.
- SY Ho, D Sanchez-Quintana, JA Cabrera, and RH Anderson. Anatomy of the left atrium: implications for radiofrequency ablation of atrial fibrillation. *Journal of Cardiovascular Electrophysiology*, 10(11): 1525 – 1533, 1999. ISSN 1045-3873.

- Meleze Hocini, Siew Y. Ho, Tokuhiro Kawara, Andre C. Linnenbank, Mark Potse, Dipen Shah, Pierre Jais, Michiel J. Janse, Michel Haissaguerre, and Jacques M.T. de Bakker. Electrical conduction in canine pulmonary veins: Electrophysiological and anatomic correlation. *Circulation*, 105(20):2442–2448, 2002. doi: 10.1161/01.CIR.0000016062.80020.11. URL <http://circ.ahajournals.org/cgi/content/abstract/105/20/2442>.
- Vincent Jacquemet. *A biophysical model of atrial fibrillation and electrograms : formulation, validation and applications*. PhD thesis, Lausanne : EPFL, 2004.
- James P. Keener. An eikonal-curvature equation for action potential propagation in myocardium. *Journal of Mathematical Biology*, 29:629–651, 1991. ISSN 0303-6812. URL <http://dx.doi.org/10.1007/BF00163916>. 10.1007/BF00163916.
- Wanda Krassowska and J.C. Neu. Homogenization of syncytial tissues. *CRC Crit. Rev. Biomed. Eng.*, 21(2):137–199, 1993.
- Simon Labarthe, Edward Vigmond, Yves Coudière, Jacques Henry, Hubert Cochet, and Pierre Jais. A computational bilayer surface model of human atria. In *FIMH 2013 - 7th International Conference on Functional Imaging and Modeling of the Heart*, Lecture Notes In Computer Sciences, London, United Kingdom, March 2013. S.Ourselin, D.Ruecker, N.Smith, Springer. URL <http://hal.inria.fr/hal-00802104>.
- Jacques Louis Lions. *Perturbations singulières dans les problèmes aux limites et en contrôle optimal*. Springer, 1973.
- Chamakuri Nagaiah, Karl Kunisch, and Gernot Plank. Optimal control approach to termination of re-entry waves in cardiac electrophysiology. *Journal of Mathematical Biology*, 67(2):359–388, 2013. ISSN 0303-6812. doi: 10.1007/s00285-012-0557-2. URL <http://dx.doi.org/10.1007/s00285-012-0557-2>.
- Stanley Nattel. New ideas about atrial fibrillation 50 years on. *Nature*, 415(6868):219–226, January 2002. ISSN 0028-0836. URL <http://dx.doi.org/10.1038/415219a>.
- M. Potse, B. Dube, J. Richer, A. Vinet, and R.M. Gulrajani. A comparison of monodomain and bidomain reaction-diffusion models for action potential propagation in the human heart. *Biomedical Engineering, IEEE Transactions on*, 53(12):2425–2435, dec. 2006. ISSN 0018-9294. doi: 10.1109/TBME.2006.880875.
- Myriam Rioux. *Numerical Computations of Action Potentials for the Heart-torso Coupling Problem*. PhD thesis, University of Ottawa, 2012.
- MARTIN ROTTER, LAM DANG, VINCENT JACQUEMET, NATHALIE VIRAG, LUKAS KAPPENBERGER, and MICHEL HAÏSSAGUERRE. Impact of varying ablation patterns in a simulation model of persistent atrial fibrillation. *Pacing and Clinical Electrophysiology*, 30(3):314–321, 2007. ISSN 1540-8159. URL <http://dx.doi.org/10.1111/j.1540-8159.2007.00671.x>.
- Stanley Rush and Hugh Larsen. A practical algorithm for solving dynamic membrane equations. *Biomedical Engineering, IEEE Transactions on*, BME-25(4):389–392, 1978. ISSN 0018-9294. doi: 10.1109/TBME.1978.326270.
- Tsukasa Saito, Kenji Waki, and Anton E. Becker. Left atrial myocardial extension onto pulmonary veins in humans: anatomic observations relevant for atrial arrhythmias. *Journal of cardiovascular electrophysiology*, 11:888–894, 2000.

- N.G. Sepulveda, B.J. Roth, and J.P. Wikswo Jr. Current injection into a two-dimensional anisotropic bidomain. *Biophysical Journal*, 55(5):987 – 999, 1989. ISSN 0006-3495. doi: DOI: 10.1016/S0006-3495(89)82897-8. URL <http://www.sciencedirect.com/science/article/B94RW-4V8RX62-J/2/02b8586e1903603f58400399b773c2bb>.
- Leslie Tung. *A Bi-Domain Model for describing Ischemic Myocardial D-C Potentials*. PhD thesis, MIT, 1978.
- Frederick J. Vetter, Stephen B. Simons, Sergey Mironov, Christopher J. Hyatt, and Arkady M. Pertsov. Epicardial fiber organization in swine right ventricle and its impact on propagation. *Circulation Research*, 96(2):244–251, 2005. doi: 10.1161/01.RES.0000153979.71859.e7. URL <http://circres.ahajournals.org/content/96/2/244.abstract>.
- Edward Vigmond, Simon Labarthe, Hubert Cochet, Yves Coudière, Jacques Henry, and Pierre Jais. A Bilayer Representation of the Human Atria. Pre-print. Paper to be presented in EMBC 2013, Osaka, Japan, June 2013. URL <http://hal.inria.fr/hal-00837671>.
- Christian W. Zemlin, Bogdan G. Mitrea, and Arkady M. Pertsov. Spontaneous onset of atrial fibrillation. *Physica D: Nonlinear Phenomena*, 238(11-12):969 – 975, 2009. ISSN 0167-2789. doi: DOI:10.1016/j.physd.2008.12.004. URL <http://www.sciencedirect.com/science/article/B6TVK-4V761XR-1/2/d4f6ced0af2780ad4f05f0b26f6a61c3>. Nonlinear Waves in Excitable Media: Approaches to Cardiac Arrhythmias, International Workshop on Non-Linear Dynamics in Excitable Media.



**RESEARCH CENTRE
BORDEAUX – SUD-OUEST**

200 avenue de la Vieille Tour
33405 Talence Cedex

Publisher
Inria
Domaine de Voluceau - Rocquencourt
BP 105 - 78153 Le Chesnay Cedex
inria.fr

ISSN 0249-6399